CHAPTER 4

STUDY OF ECCENTRIC SCREW ON VASCULAR INJURY DURING TOTAL HIP REPLACEMENT

4.1 Introduction

Incidence of minimally invasive total hip arthroplasty (MI-THA) has remained increasing for past 25 years in orthopedics as a result of the rapid upgrade of materials and instrumentation (T Cheng et al, 2009; T.P. Sculco, 2004). In the past few years, enormous modifications have occurred in the techniques of exposure for THA, increasing the demand for carrying out THA by mini-incisions (MI). Since, minimally invasive THA incorporates the use of internervous planes for a modified surgical dissection that reduces trauma to any tendon or muscle throughout the exposure, thus allowing hip replacement to be completed by less invasive exposures and attain outstanding results. T. P. Sculco reported that the modified approach of posterolateral technique is best suited, and length of skin incision is between 7 and 10 cm in most patients. He proposed the rationale for carrying out minimally invasive hip arthroplasty and concluded its importance such as reduced stay at hospital, fast retrieval, reduced loss of blood, and decreased trauma during surgery. With the use of larger and more radical dissections, there are frequent risks of trauma to the soft tissues with the implication of standard approaches for hip surgery. He therefore, insisted on performing safe hip arthroplasty surgery through incisions of 6-10 cm without increasing the injury to the patient and without compromising with the result of arthroplasty. T. Cheng et al performed a study for comparing the operative consequences between standard and mini incisions during total hip arthroplasty (THA). They evaluated the variances in results for different surgical approaches, experimental quality, and follow-up period by subgroup as well as sensitivity analyses and concluded that blood loss and operative

time reduced significantly during the mini-incision technique performed with the posterolateral or posterior approach.

During MI-THA, laceration of major blood vessels during fixation of the screw has been reported. Avisar et al performed a 16-year retrospective analysis in order to investigate the possibilities of vascular complications during total knee arthroplasty (TKA) and total hip arthroplasty (THA). They stated a total of six cases of vascular injury requiring specialist intervention. Out of 2073 total TKRs, one case of popliteal artery injury, one case of venous injury and two cases of lateral geniculate artery injury were reported (Avisar et al., 2015). Whereas, two cases of arterial injury were reported from 1601 THRs. A study on the acetabulum was perforfed by S. K. Hwang (Hwang et al., 1994) so as to define the safe zones for fixation of transacetabular screw. They observed a substantial retroperitoneal blood loss because of a perforation in external iliac vein during total hip surgery with a bone graft fixation to the acetabulum with screws. The study suggested that good bone stock was available at postero-inferior and postero-superior quadrants of acetabulum and were considered safe for the transacetabular screw fixation. Also, the antero- inferior and superior quadrants should not be considered for screw placement in these quadrants because it may damage the obturator vessels or the external iliac vein and artery. R. L. Barrack studied the complications of injury to neurovascular structures in total hip replacement (THR) and concluded that most common nerve injury is partial sciatic palsy (Barrack, 2004). Further, the injury to vascular structures occurs mainly due to the placement of screws to fix acetabulur components, structural grafts, and protrusio cages or rings. J. Parvizi et al. also studied and evaluated the outcomes of vascular injuries after joint surgery (J.

Parvizi et al., 2008). Out of the collected data of 13,517 patients experiencing total joint arthroplasty, a total of 16 vascular damages were reported. 11 injuries after total knee replacement (TKR) and five after total hip replacement (THR) were noted. Indirect injury was observed as the most common mechanism in TKR. Whereas, direct injury was most common in THA. A case report presented by Kong et al, reported a delayed presentation of injury to iliac artery due to acetabular screw (Kong et al., 2013). They observed an unexpected loss of blood while performing a screw extraction from an uncemented acetabular shell at liner revision that was 10-year-old. Further reducing the chance of hemorrhage by replacing the screw, but revealed an injury caused by the screw in internal iliac artery. Thus, they suggested that performing imaging techniques preoperatively helps to reduce the risk, and emphasized on the requirement of preoperative imaging during revision surgery. However, fixation of the screw is a critical procedure: correct alignment of a sized screw placed in the right direction and position will avoid vascular injury (Dietze et al., 2014). As proposed by Wasielewski et al, (Wasielewski et al, 1990) the safest zones for the transacetabular screw fixation in the acetabulum during uncemented acetabular surgery limited the intrapelvic injury. Since these structures were not perceptible to surgeon during screw placement, cadaveric studies had to be performed in order to locate these structures with fixed points of reference inside the acetabulum. The acetabulum was divided into four clinically useful quadrants by drawing two lines dividing acetabulum in halves, forming four quadrants. Each screw fixed on the cup fell into one of the four quadrants. The distance between the screw tips and vascular structures were measured and considered safe or endangered. The study revealed that posterior inferior and posterior superior

acetabular quadrants comprise a maximum bone stock and are therefore relatively safe for the transacetabular screw fixation. Whereas, the anterior inferior and anterior superior quadrants whenever possible must be avoided, because improper screw placement in these observed quadrants may threaten the obturator artery, along with the external iliac vein and artery, nerve, and vein.

However, with recent advancement in the design and manufacture of hip implants, manufacturers are providing acetabular cups with eccentric holes. Due to the modifications in acetabular cups with eccentricity of holes (up to 34°), new eccentric screws are being manufactured rapidly. Consequently, performing hip arthroplasty surgery with these modern acetabular cups containing eccentric holes followed by eccentric screw fixation imposes a great threat of vascular injury if the anatomical guidelines proposed by Wasielewski et al. are taken into consideration.

There is an immediate requirement of modification in the anatomical guidelines proposed by Wasielewski et al. so that the modified quadrant system of acetabular region aids the surgeon to obtain a simple intraoperative guide for the safe transacetabular screw placement while performing primary as well as revision acetabular arthroplasty.

Therefore, the goal of this study is to obtain spatial information of angular screw eccentricity that affects the vascular structure's proximity to pelvis bone and possible angular screw eccentricity which is tolerable and for due consideration.

4.2 Anatomy of pelvic bone and neuro-vascular structures:

4.2.1 Pelvis structure:

The three-dimensional anatomy of pelvis is complex and often hard to understand. A lot of vital vascular and neural structures are present within and immediately around the pelvis bone. The bony pelvis is made up of the ilium, ischium, and pubis (Figure 4.1). The acetabulum is present at the junction of these three bones. A ring of bone that connects the torso to lower limbs is formed by a combination of these bones when they unite posteriorly to the sacrum and anteriorly at the pubic symphysis.

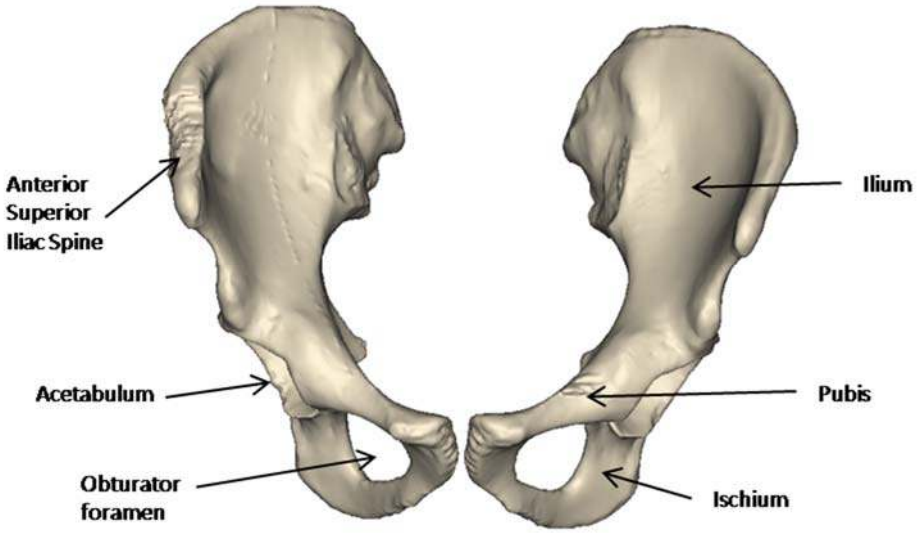

Figure 4.1: Schematic showing anatomy of the pelvic region

4.2.2 Vascular structures

Understanding the exact location of vessels is important for complex revision THA because of extensive exposure of acetabulum. The important vessels that are present

inside and around the pelvis include the external and internal iliac, obturator, internal pudendal, femoral, and inferior and superior gluteal vessels.

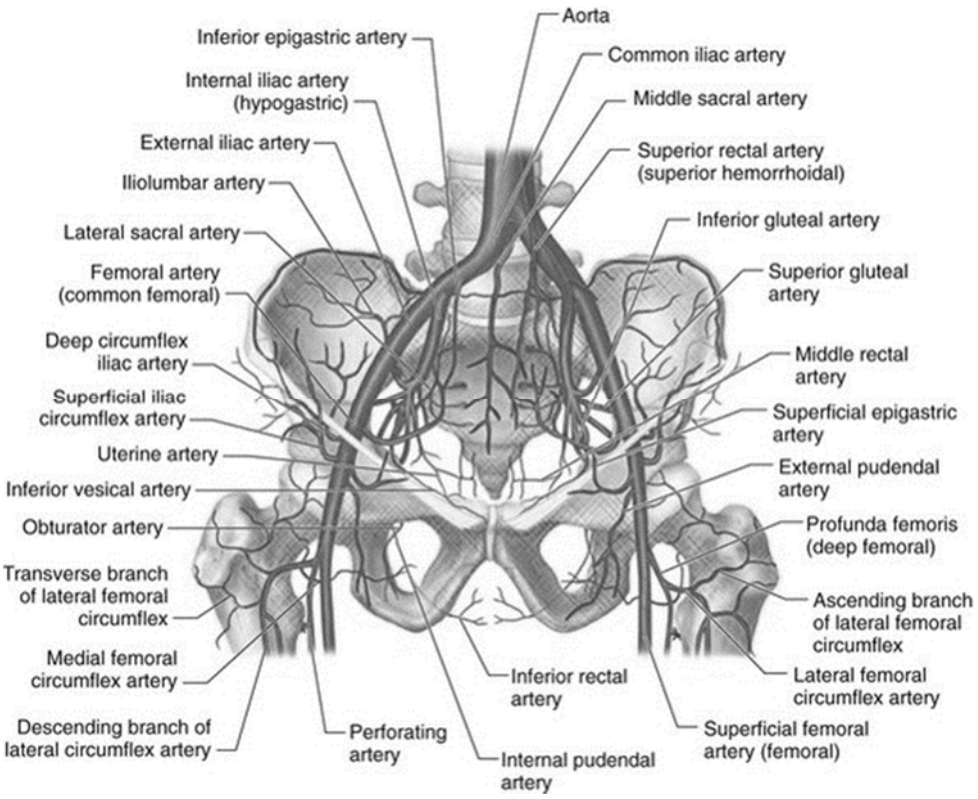

Figure 4.2: Complete vessel anatomy of pelvis region

At L5-S1 vertebral disk, the common iliac artery is divided. The external iliac artery dividing anteriorly, continues distally and becomes the common femoral artery. Whereas, the posterior division converts into the internal iliac artery. Again, the internal iliac artery further splits to divide posteriorly and emerges into the superior gluteal artery, whereas an anterior division leads to form the obturator artery the obturator artery again branches into internal pudendal artery and the inferior gluteal artery. The external iliac vein and artery lie close to the pelvis and are immobile (Figure 4.2). The external iliac vein lies at the acetabular dome within 4 mm and has been shown to lie at the anterior column of the pelvis within 7 mm at the anterior inferior iliac spine. It is

located at the anterior inferior iliac spine within 10 mm of the bone and at the acetabular dome within 7 mm. The common femoral artery occurs anterior and medial to the hip region. At this point, only the iliopsoas is present between the hip capsule and vessel. The femoral vein is located medial to the artery (Figure 4.3). The obturator vessels are present at the quadrilateral surface and occur within 1 mm of the bony surface, and therefore the interpositioning of the obturator internus muscle is their only protection.

The superior gluteal vessels are located at an average distance of 5 mm from the sciatic notch. Whereas, the inferior gluteal vessels are observed at a distance of 6 mm and the pudendal vessels are present at a distance 12 mm from the posterior column, at the ischial spine. Both, well protected by a layer of fat and are mobile (E.M. Keating et al, 1990). Additionally, the deep femoral artery divides to form the lateral and medial femoral circumflex arteries.

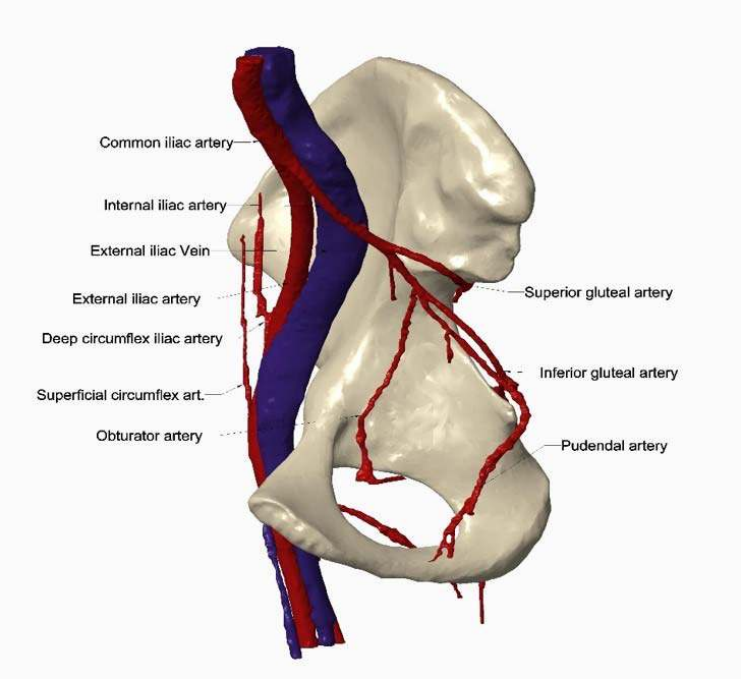

Figure 4.3: Developed schematic of pelvis along with its associated neural and vessel anatomy

4.2.3 Neuroanatomy

The femoral, sciatic, obturator and superior and inferior gluteal are the primary nerves of the pelvic region. The most lateral structure inside the femoral triangle is the femoral nerve. It is located on the psoas muscle belly between the pubic tubercle and anterior superior iliac spine at the midpoint, approximately. It is anteriorly related to the acetabulum. The superior gluteal nerve is generally well protected because of the greater trochanter and passed through the gluteus medius and minimus muscles (Figure 4.3). The inferior gluteal nerve is present inside the gluteus maximus proximally and medially in the area. The obturator nerve progress with the obturator vessels (Hoppenfeld et al., 1994).

The sciatic nerve was observed nearest to the posterior column at an approximate distance of 9 mm in pelvis at the acetabular dome as reported in a normal computed tomography (CT) review. Also, it was more protected at the ischial spine. The nerve was at an approximate distance of 15 mm from the ischial spine due to the presence of short external rotator muscles between the nerve and bone at this point (Wasielewski et al., 1990).

4.3 Neuro-vascular injury in THR:

The risk for injury during acetabular surgery varies in accordance with the contiguity of the major vessels to bone. Massive hemorrhage resulting in immediate exsanguination may be caused due to the damage of any of these vessels by processes such as drilling, reaming, retraction, or dissection. The external iliac vein and artery are closely related to the pelvis lie immobile, and are therefore at highest threat for injury during THA. Due to its thicker intima of external iliac artery and larger distance from

the bone it is not as much of the risk. The femoral vein is less likely to be damaged as it is located medially to the artery. The obturator vessels are only protected by the interposition of the obturator internus muscle and therefore are also at risk (Figure 4.4). The superior gluteal vessels are at highest risk at the sciatic notch, but have been reported to experience less injury as a complication of THA. Since, the lateral and medial femoral circumflex arteries are situated near femoral neck, so are vulnerable to retractors.

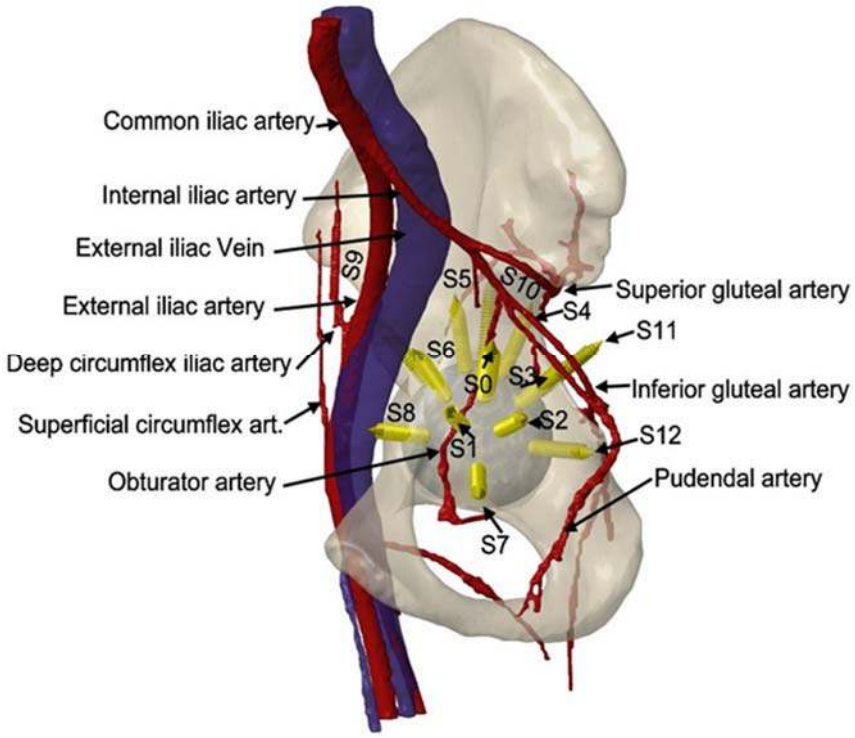

Figure 4.4: Effect of screw fixation on the neuro-vascular structure

The peroneal branch of the sciatic nerve suffers with most common nerve injury during hip surgery and is further trailed by obturator, superior gluteal, and femoral nerves. Functional loss as well as poor consequences are experienced by the patients as a result of injury to these structures. Dissection of capsule puts the femoral nerve at a higher

risk as compared to drilling or reaming. The superior gluteal nerve is generally well protected as long as the dissection does not extend >5 cm above the greater trochanter (Ramesh et al., 1996). Since, the inferior gluteal nerve is located inside the gluteus maximus proximally and medially in the area and is split while undergoing posterior approach to the acetabulum, it is at lesser risk of injury (Figure 4.4). Injury to sciatic nerve is most common during THA (Schmalzried et al., 1991). It is assumed that out of several conjectural reasons for the most common cause of injury to the sciatic nerve is its anatomic location.

4.4 Surgical approaches to the acetabulum during THR

The most common surgical approaches to acetabulum during total hip surgery include posterior and anterolateral approaches (Figure 4.5). Excellent visualization is provided by both the approaches to reach the acetabulum. Lateral approaches provide more exposure as compared to the posterior oriented approaches, still we find the posterior approaches to be more popular than the lateral. The anterior and ilioinguinal approach are also defined since these approaches are provide more extended exposures (Ramesh et al., 1996). Generally, the surgical approach decided for acetabular modification is probably going to be the same as that utilized for the essential surgery unless different factors are included, such as, the requirement for more exposure.

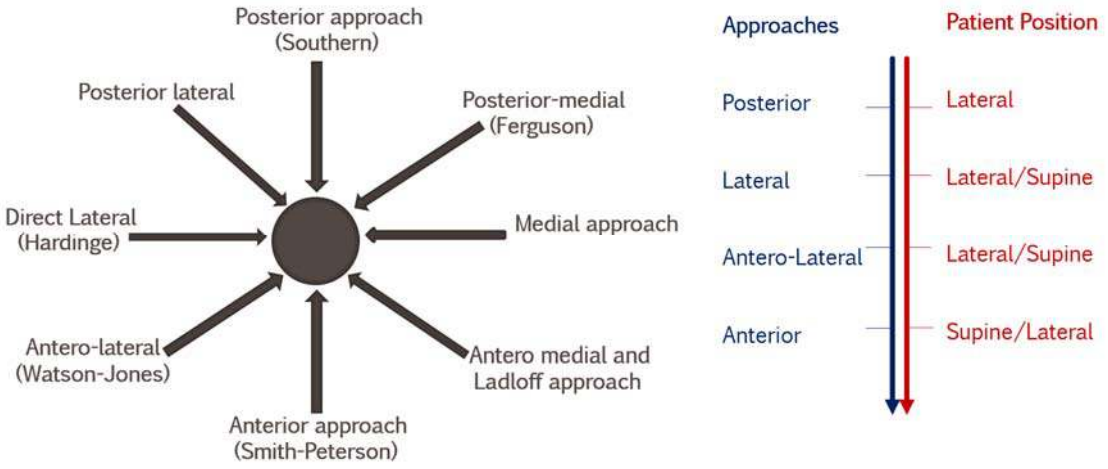

Figure 4.5: Surgical approaches with respect to the patient position during Total Hip Arthroplasty.

4.4.1 Posterior approach

The least demanding surgical approach for THA is the posterior approach. Good visualization is provided by this approach to reach the acetabulum, particularly of the posterior wall when the patient is positioned laterally. This is the most commonly used approach in the United States for THA. No internervous plane is located since splitting of the gluteus maximus occurs in line with its fibers during this approach. The short external rotators preserve the sciatic nerve once they are detached from their attachments on the femur and reproduced medially (Figure 4.6).

The posterior approach imposes the major vascular risk leading to the damage of the inferior gluteal artery. This vessel is intramuscularly branched, which are often damaged during splitting up of the gluteus maximus, hence they must be clearly visualized and prevented during dissection. For trauma surgeon treating intricate pelvic fractures including the greater sciatic notch, a risk to the inferior gluteal artery also exits just below the pelvis in the lower region of the piriformis.

The contusion of sciatic nerve is the major nerve injury that occurs during the posterior approach. Avoiding extreme traction and confirming proper nerve protection with short external rotators might reduce the damage to large extent. The risk of injury may also be decreased by preserving the nerve out of the operative field while retaining the hip in an extended position. No attempt should be made to dissect the nerve from its neighboring perineural fat, unless indicated specifically.

4.4.2 Anterolateral approach and modifications

A common approach is that of anterolateral approach for THA. The exposure provided by this approach to the acetabulum excellent. And the dissection is performed by the intermuscular plane of the gluteus medius and tensor fascia lata by positioning the pateient laterally (Figure 4.6). An osteotomy of trochanter is preferred by some surgeons, while others prefer to detachment of the two-thirds of the anterior of gluteus medius from its insertion on the greater trochanter.

The Hardinge is a modification to this approach where the two-thirds of anterior of the gluteus medius is detached and continued with a soft tissue sleeve including a splitting of the proximal vastus lateralis (Hoppenfeld et al., 1994).

The laceration of femoral artery and vein is the main consequence associated with the anterolateral approach. These are vulnerable to retractors when located too far anteriorly. The placement of anterior retractor should be positioned at 1-O'clock direction for right hip and at a position of 11 O'clock for the left hip. Care must to be taken to guarantee that the tip of the retractor is set directly on bone and does not puncture the psoas muscle as it is the only protection for femoral vessels barrier in the

acetabulum. Another alternative to this method is to pass a retractor which is curved bluntly into the pelvis at the acetabulum anteriorly. The femoral nerve is susceptible to retractors and excessive retraction since it is placed laterally in the femoral triangle. Splitting the gluteus medius in order to modify this approach imposes a great risk on the superior gluteal nerve (Hoppenfeld et al., 1994).

While splitting vastus lateralis, the transverse division of the femoral circumflex artery present laterally may be observed during this approach and therefore must be prevented.

4.4.3 Anterior approach and modifications

This approach provides access to the anterior lip and anterior column of the acetabulum and is mainly used for open reduction in case of developmental hip dislocations. The supine positioning is used to place the patient. The dissection performed superficially results in the exploitation of the internervous plane present between the femoral nerve and superior gluteal nerve. The identification and protection of femoral cutaneous nerve present laterally can be obtained as it appears above the sartorius, at an average of 2.5 cm present inferiorly to the anterior superior iliac spine. A plane between the rectus femoris and gluteus medius is used to perform a deep dissection. The femoral vessels and nerves, during dissection are at higher risk, because they are anteriorly related to the hip. The protection of femoral structures is ensured only if the superficially arrangement of plane of sartorius and tensor fascia latae as well as a more profound arrangement of gluteus medius and rectus femoris is maintained during the dissection. The femoral circumflex artery present laterally with its further division must be coagulated as it passes through the operative field at the interval between the sartorius and tensor fascia latae, proximally.

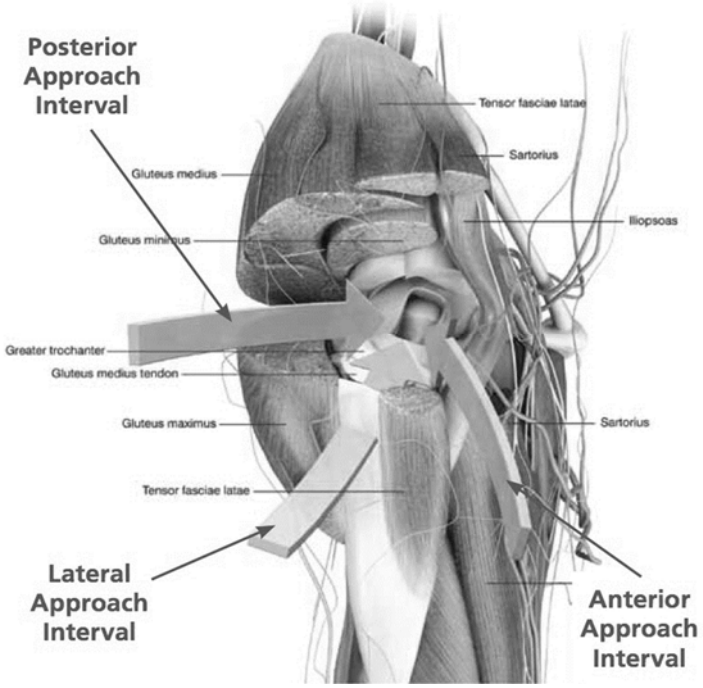

Figure 4.6: Conventional approaches for hip replacement. (a) Posterior (b) Lateral (c) Anterior approach interval.

An increased exposure of the anterior column and medial wall can be obtained when the incision is made on the origin of the sartorius located at anterior superior iliac spine as well as the head of the rectus at the anterior superior iliac spine, directly (Smith-Petersen et al., 1931). This approach was modified by incising the tensor fascia latae placed distally from the myofascial portion in order to reach the trochanteric region and femoral neck. A modified anterior approach is described by Light and Keggi, (TR Light et al., 1980) which protects the femoral cutaneous nerve placed laterally and to reduce complications to nerves during THA when a dissection made laterally so as to provide a muscle cuff splits the medial fibers of the tensor fascia latae medially.

4.4.4 Ilioinguinal approach

This approach provides better visualization of the inner surface of pelvis and medial wall and anterior column of acetabulum. It is useful for acetabular fractures involving

the anterior column, anterior wall as well as allied posterior and anterior hemi-transverse fractures, and transverse fractures as presented in figure 4.7.

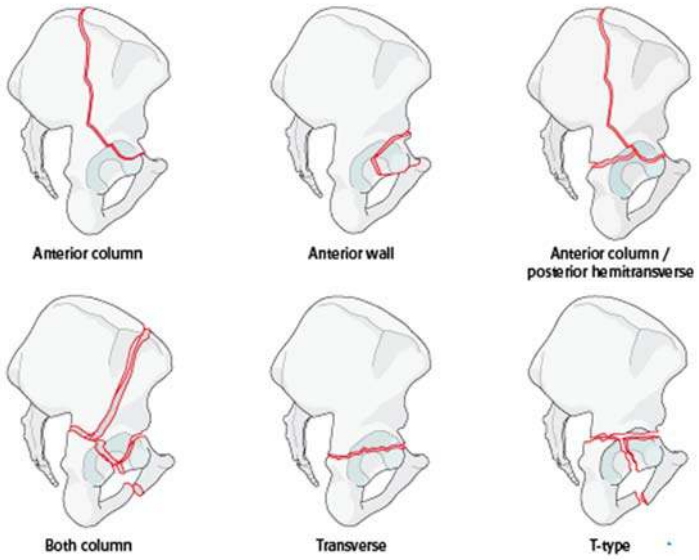

Figure 4.7: Types of acetabular fractures

This approach has many advantages that include: fast recovery, outstanding cosmesis, and decreased heterotopic formation of bone as compared to further approaches. The subject is positioned in supine arrangement for this approach. The main objective of this approach is to cut narrowly along inside wall of pelvis and pick up each neurovascular and muscular structure without destroying it. This approach consists of three windows, each helping to reach different structures. The first window permits contact to the sacroiliac joint anteriorly, upper portion of anterior column and iliac fossa internally. Second window present in between the iliopsoas and iliac vessels, permits entry to the brim of pelvis, and pubic ramus superiorly and quadrilateral surface. Third window permits reach to superior ramus, pubic symphysis, retropubic space and the quadrilateral surface.

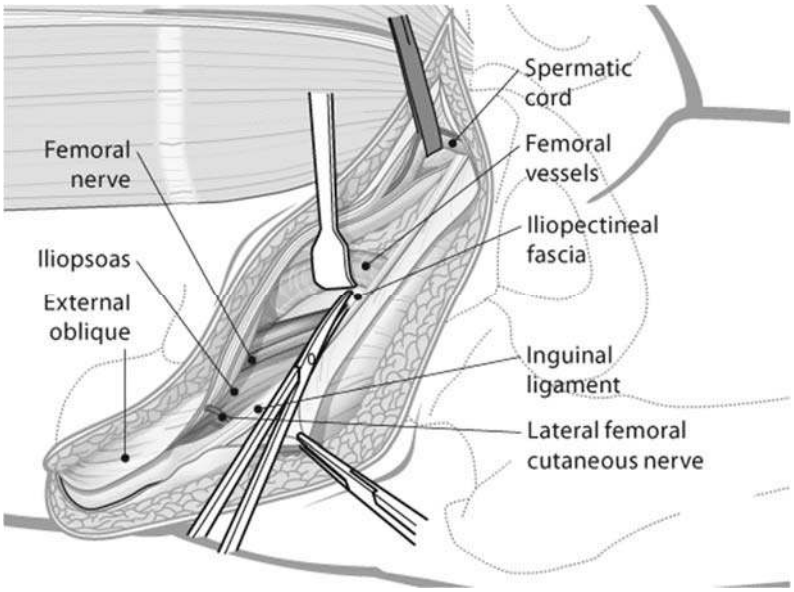

Figure 4.8: Ilioinguinal approach to hip joint during hip surgery

During this approach, the endangered nerves are: femoral nerve lying below the inguinal canal on the iliopsoas muscle anteriorly. It may be damaged by the retraction or injured during the dissection. The cutaneous nerve of the lateral femur is branched at the superior iliac spine anteriorly if otherwise retracted easily without tension. As described previously, the femoral vessels proceed mediallly to the iliopectineal fascia and thus are endangered. The inferior epigastic artery must be preserved as it islocated medially at the inguinal ring at depth. Other structures like the bladder, bowel, and spermatic cord are also likely to be damaged.

4.5 Quadrant system used in THR

As proposed by Wasielewski et al, a concept of quadrant system was designed for considering screw placement in a safe zone so as to prevent major injury to vascular structures in its vicinity. Two lines A and B drawn perpendicular to each other split the acetabulum into four quadrants as shown in the figure 4.9. Line A extending from the region of anterior superior iliac spine (ASIS) passing centrally through the acetabulum

up to the posterior portion of fovea, divides the acetabulum in two quadrants. Line B made perpendicular to Line A at mid-point of acetabulum divides it in four respective quadrants namely: the anterior-inferior quadrant, anterior-superior quadrant, posterior-superior quadrant and posterior-inferior quadrant.

The posterior-inferior and posterior-superior quadrants contain the thickest bone and maximum potential in order to obtain secured fixation imposing minimum risk of injury to vessels in cadaveric studies. The anterior-inferior quadrant and anterior-superior quadrant considered as the quadrant of death were observed as the most dangerous quadrants for placement of screw due to the presence of thin bone and close vicinity of the vessels to bone in that region (Figure 4.10).

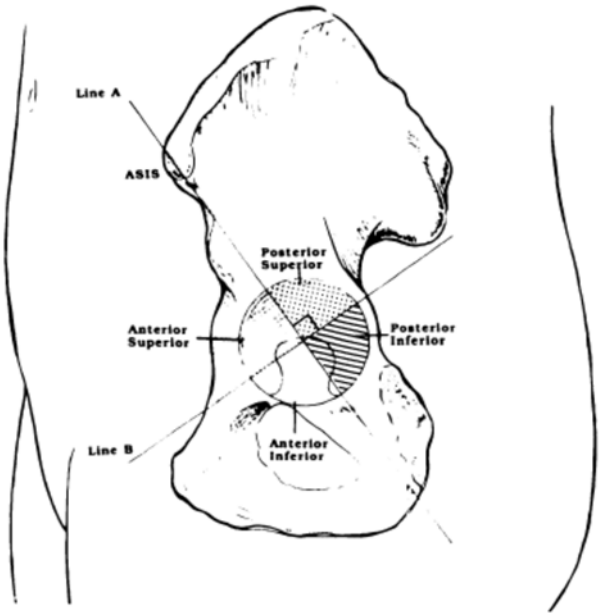

Figure 4.9: Schematic of the quadrant system proposed by Wasielewski et al. for screw fixation in safe zone. (Reprinted with permission from Wasielewski et al. 1990)

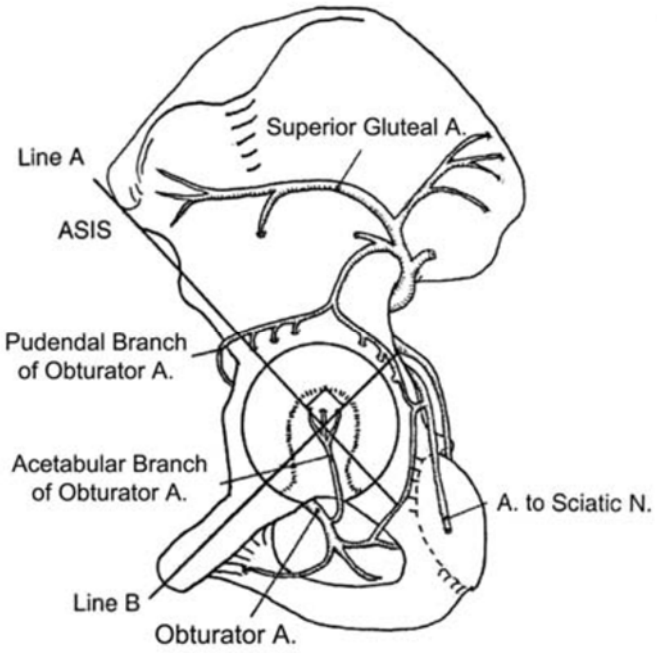

Figure 4.10: Illustration of superimposed acetabular quadrant system along with intrapelvic vessels as defined by RC Wasielewski et al., 1990 Reprinted with permission from Wasielewski et al. 1990)

4.6 Objectives

The quadrant system is used to avoid injury to vessels and intrapelvic structures that are not clearly visualized to the surgeon during screw fixation.

Quadrant system was developed in 1990. Formerly, no such acetabular cups with angled holes were manufactured. However, in recent years' cups are manufactured with angled holes, due to this, rotation of screws occurs up to 34° which would cause a potential risk for vessels proximal to pelvic bone.

Yet no anatomical guidelines or modified quadrant system has been developed to fix the angular eccentric screws during THA. Therefore, we shouted to obtain spatial

information of angular eccentric screws that affects the vascular structures proximal to pelvis bone.

4.7 Workflow

A flow chart indicating step by step work and software required to carry out each step is shown below in Figure 4.11.

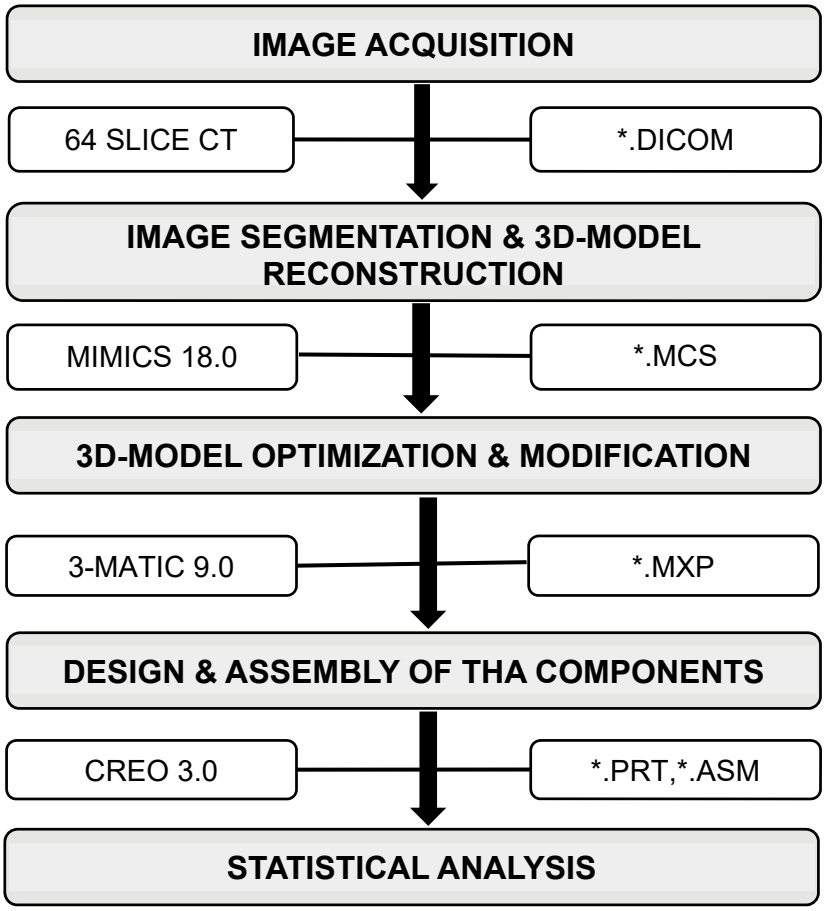

Figure 4.11: Flowchart describing the progress of work with associated software

4.8 Building a 3D pelvis model

The creation of the 3D pelvis model used in this study was originally done through Mimics 18.0 and 3-Matic softwares (Materialise, Leuven, Belgium) by processing medical images. The main stages of model creation are: collection of CT scan data (image acquisition), generation of anatomical structures from CT scans (image

segmentation, 3D model reconstruction and optimization), development of CAD model of Total Hip Implants & screws (design and assembly of THA components).

4.8.1 Data acquisition:

To generate a model of a specific anatomical structure it is essential to identify the tissues that compose the organs. Then, an appropriate medical imaging modality is selected for data acquisition according to the desired image features. In previous studies, either a wet bone, synthetic bone, a frozen (dry) bone, or an apparent density of bone was used for the analysis but in computational biomechanics, especially for orthopedic applications, CT has been increasingly adopted for bone remodeling since hard tissue has a high contrast relative to soft tissue like cartilage, muscles, ligaments, etc. (L. Peng et al., 2007). It is well known that CT data provides a fairly precise quantitative information on geometry of bone and the bone tissues associated with its mechanical properties. For all cases here reported CT imaging is the proper selection.

CT images represent a map of pixel containing the tissues with a linear X-ray attenuation coefficient (Nareliya et al., 2011). Each pixel value is scaled in a manner such that the linear X-ray attenuation coefficient of air is equal to -1000 and that of water is equal to 0. This scale is known as Hounsfield scale (HU) or CT numbers (Figure 4.12) named after one of the pioneers in CT, Godfrey Hounsfield. It is a quantitative scale for describing radio density, can be calculated as:

$$HU = 1000(\mu_x - \mu_{water})/\mu_{water}$$

Where, μ_x = Average linear attenuation coefficient in a voxel, μ_{water} = Linear X-Ray attenuation coefficient of water

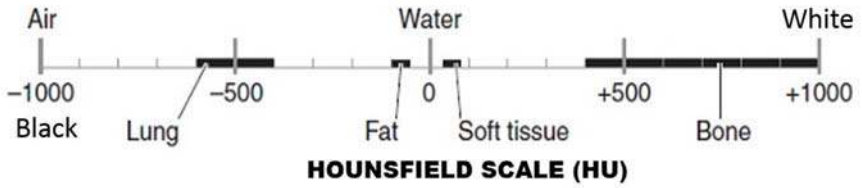

HOUNSFIELD SCALE (HU)

Substance	HU
Air	−1000
Lung	−700
Soft Tissue	−300 to -100
Fat	−84
Water	0
CSF	15
Blood	+30 to +45
Muscle	+40
Bone	+700(cancellous bone)to +3000 (dense bone)

Figure 4.12: Hounsfield scale showing a range of Hounsfield Unit for body system

A 64 slice CT scanner, GE Medical System was used to acquire CT images by aligning the lower extremity of the patient to the CT scanner rotating in clockwise direction. The images obtained were in DICOM format (Digital Imaging and Communication in Medicine) and imported directly to Mimics (**M**aterialise's **I**nteractive **M**edical **I**mage **C**ontrol **S**ystem) which is a Materialise's software for medical image processing and 3D modelling.

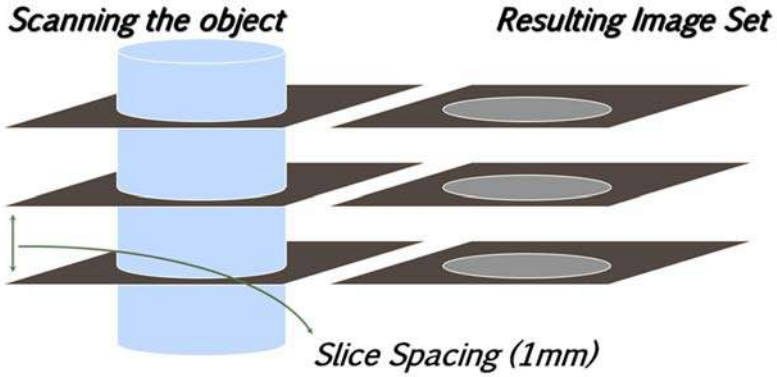

Figure 4.13: Schematic illustrating the process of data acquisition

Mimics makes use of 2D cross-sectional medical images from imaging modalities such as computed tomography (CT) to build 3D models, which can be directly linked with CAD software for surgical simulation and FE analysis (Figure 4.13). An acquired set of images can be directly imported in the Mimics software which usually contains images in XY plane (axial images). Further, it calculates and constructs images in XZ (coronal) and YZ (sagittal) direction which facilitates a more precise 3D appearance of the 2D data.

The DICOM patient based coordinate system is a coordinate system which is right handed. The X-axis increases to left side of patient whereas the Y-axis proceeds to posterior side and the Z-axis moves towards the patient head.

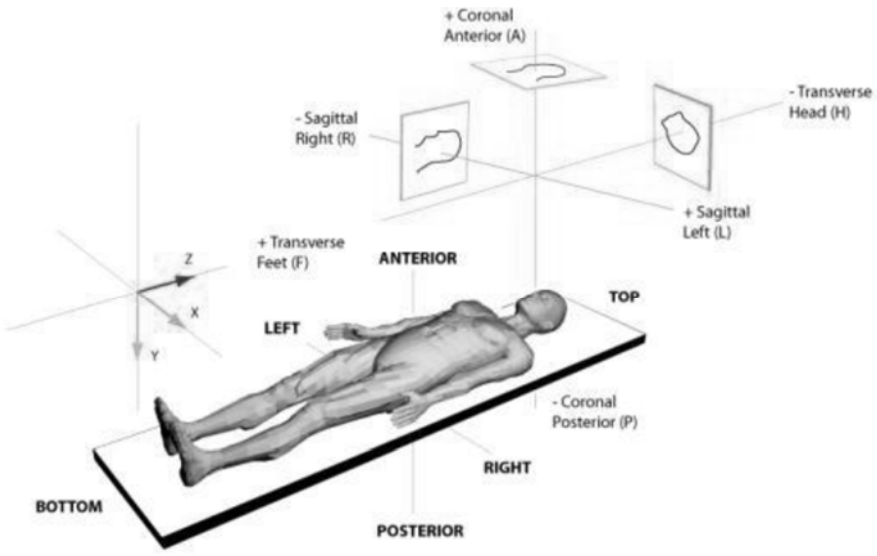

Figure 4.14: DICOM patient based coordinate system

4.8.2 Obtaining material properties from CT-data

Previous studies have concluded that the relationship between Hounsfield Units (obtainable from greyscale data) and mechanical properties are strong enough to

support use in FE (Les et al., 2005). Ideally, a phantom is scanned at the same time as the subject, so that a correlation between apparent density and Hounsfield Units for the CT-data can be found (Taddei et al., 2007). Material stiffness can then be related to the apparent density based on experimentally derived relationships, of which there are many. If no phantom is available, the relationship between apparent density and Hounsfield Units can be estimated from inspection of the CT-data to ascertain the limits of cortical and trabecular bone (Majumder et al., 2007). No phantoms were available in the CT-scans used in this study. Most density stiffness relationships focus only on trabecular bone, but some cover the cortical region as well. Helgason et al. in 2008, noted substantial inter-study differences in their comparative review of all predictive relationships, although this was based on studies that focused on different bones in the body so differences can be expected.

4.8.3 Preparing the acquired CT Data:

In presence of signal noise and image artifacts it is necessary to improve the resolution and quality of the CT images by appropriate acquisition parameters tuning as slice thickness and spatial resolution. Also, several digital image processing techniques can be applied in order to enhance the visual information contained in an image.

Windowing:

The gray values of CT images are expressed according to the Hounsfield scale shown below, which has 4096 values. To map this scale onto the 256 gray values of your computer, Mimics has a feature called windowing. Windowing is a tool to adjust the image contrast (Figure 4.15).

Figure 4.15: Difference between predefined bone scale and soft tissue scale for setting the contrast in Mimics 18.0 (Materialise, Leuven, Belgium)

Differences between soft tissue, fat, muscle as well as bone can be visualized depending on the window chosen. For best resolution, the contrast tool contains a grayscale which has certain predefined scales. Each set of scale has a fixed minimum and maximum value, enlisted in Table 4.1.

Grayscale	Minimum value	Maximum value
Custom Scale	-1024	350
Bone Scale	-1024	1590
Soft tissue Scale	-150	350
Narrow Scale	-900	1100
Wide Scale	-1024	1590
MRI Scale	-1024	-524

Table 4.1: A range of predefined Grayscale with maximum and minimum values.

Volume Rendering:

Volume rendering helps in quick visualization of 2D data as a 3D object without having to take the time to segment and create a model. It is only a visualization tool and gives a nice impression of what your model will look like. Volume rendering consumes a lot

of system memory slowing down computer processing time, so it's turned it off after visualization.

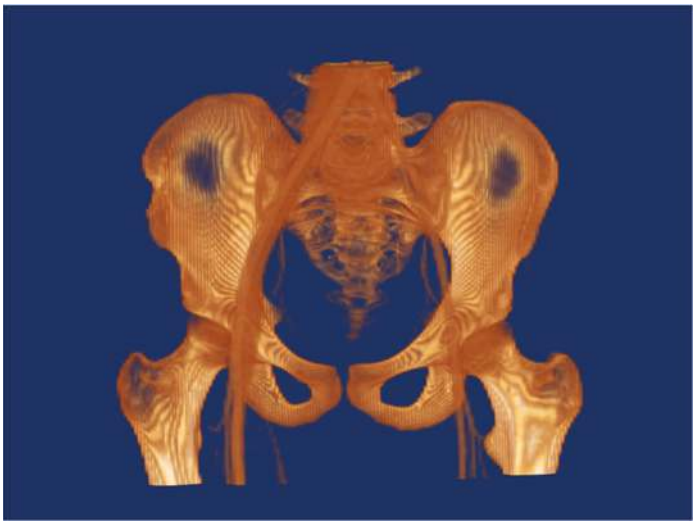

Figure 4.16: Image showing bone scale volume rendered data

4.8.4 Image Segmentation and 3D model reconstruction

Segmentation:

The process of converting anatomical data from 2D images to 3D models is a process called segmentation. For segmentation the region of interest is indicated in the sliced 2D image data. This data is further used to reconstruct a 3D model from the segmented regions. Mimics uses the STL format to define the outer boundary of 3D model. The STL format then accurately describes the most complex geometries. This is essential as the anatomical data is generally very complex. Accurate segmentation is therefore required to extract significant information from images. Segmentation plays a fundamental role for anatomical modeling as it forms the conversion of image data to 3-D mesh data. However, when dealing with medical images, segmentation is one of the most difficult tasks to be performed within the entire project. Various different segmentation methods exist and can be selected according to the input image. Taking

into account that CT images are the source of 3-D medical data for the construction of 3D pelvis model, four techniques are used in conjunction to solve the bone segmentation problem: windowing, thresholding, region growing (automatic partial segmentation) and editing mask (complete manual segmentation).

The medical images obtained from CT scanners consist of grayscale information. 3D models are created based on the grayvalues (Hounsfield units in CT images) within these images. A gray value is defined as a number which is associated with the pixel of the image describing the shade of the pixel that may be white, gray, or black. There is a direct relationship between the gray value assigned to each pixel in the image data and material density of the scanned object. The image data can be segmented by combining similar gray values leading to the construction of 3D models. This type of segmentation is called thresholding and yields accurate models.

Thresholding:

All the pixels are classified within a Hounsfield range by the same color or mask. The predefined scales are provided for some biological materials that are listed in the threshold toolbar. A low threshold value is used to segment the soft tissue, whereas a high threshold value segments the bone.

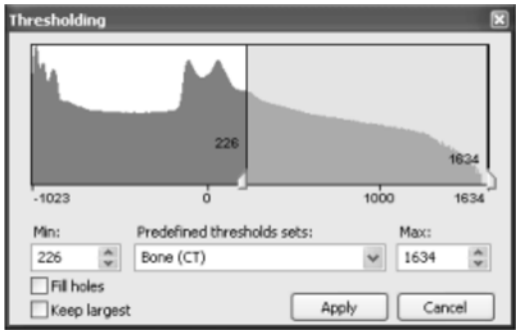

Figure 4.17: Histogram illustrating the threshold range for bone (CT)

The predefined threshold values are used to view how different thresholds highlight different areas of the images. In this case a good threshold for bone is the predefined bone (CT) setting which is 226 to 1634. Therefore, for selecting bone on CT images, the lower threshold is set on 1/3 of the cortical peak.

Region Growing:

It is an automatic partial segmentation process which separates the masks in different fragments and helps to remove the floating pixels.

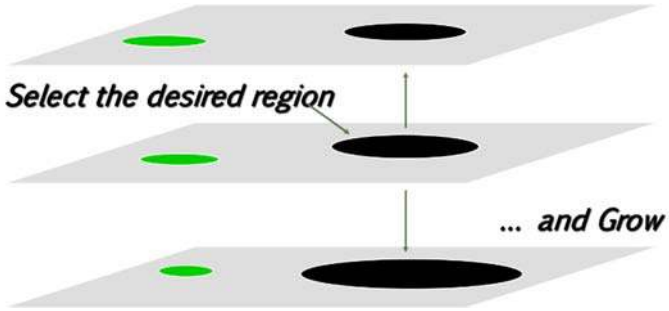

Figure 4.18: Illustration of the region grow process

The purpose of applying region growing segmentation was that, though, it does not provide complete segmentation in one go but enhances the parts near the complex regions with a new mask so that the complete region of interest can be visualized properly. This makes the next step of manual segmentation much easier.

Edit mask (manual segmentation):

All manual editing functions are performed on the active mask. In order to preserve the original geometry, it was essential to keenly observe the pixels and segment them accordingly. Manual segmentation is performed by using edit mask tool which helps to erase, draw or even reestablish the image with a certain value of threshold. This method is performed after region growing in order to achieve complete segmentation of region

of interest, resulting in a more continuous surface. Therefore, exact geometry can be extracted from the CT scan images so as to obtain a perfect 3D geometry.

Smooth Mask:

Smoothing filters, the outliners resulting from manual segmentation, while preserving important boundaries. This operation removes any artifacts present in the mask and subsequently improves the quality of surface for the developed 3D objects.

4.9 Automating the model creation

4.9.1 Data acquisition

For our study, we obtained the angiographic CT image pelvic data of thirty-eight patients (24 men, 14 women) from the Radio Diagnosis & Imaging Department, SS Hospital, BHU, after patient informed consent. All subjects were scanned with a 64-slice spiral computed tomography scanner (GE medical systems, US) and 80 ml of omnipaque iohexol was injected by intravenous process by high-pressure injector through the cubital vein as a contrast medium. Scanning parameters were predefined as: 120 kV, 270 mA, .625 mm slice width with 1 mm spacing, scanned region: third lumbar vertebra to mid of femur bone and subsequent reconstruction distance of 1 mm.

As a result, we obtained a matrix with gray scaled pixels based on tissue density in the DICOM format (Digital Imaging and Communications in Medicine), considering no subjects to be affected with pelvic and arterial trauma.

The reconstructed data was stored in .dicom format. The DICOM format is a standard in the Medical Imaging world and most recent scanners are DICOM compliant.

4.9.2 Three dimensional model reconstruction

Volumetric data were transferred to medical imaging and editing software Mimics 18.0 (Materialise, Leuven, Belgium), to reconstruct the 3D model of pelvis and vessels. Semi-automatic segmentation algorithm applied in combination with region grow algorithm was used to incorporate the 2D dicom image data, consequently leading to the reconstruction of 3D geometry (CJ Lavernia et al., 2007). Creation of rectangular patches, smoothing and filling holes on the generated 3D models was done in 3-Matic 9.0 (Materialise, Leuven, Belgium) module and stored in STEP format.

Windowing:

The contrast tool contains a grayscale which has certain predefined scales. Each set of scale has a fixed minimum and maximum value.

The contrast is set to a predefined bone scale (-1024 to 1590) for carrying out the segmentation of pelvic bone.

4.9.3 Image segmentation

The pelvic bone is segmented using image processing tools:

Thresholding:

This tool contains a predefined threshold set for varying bone densities. For thresholding the pelvic cortical bone, a predefine threshold of Bone (CT) is used which has a maximum and minimum value of 226 and 1590, respectively. The figure 4.19 (a-c) shows the effect of threshold on CT image and the threshold region of bone.

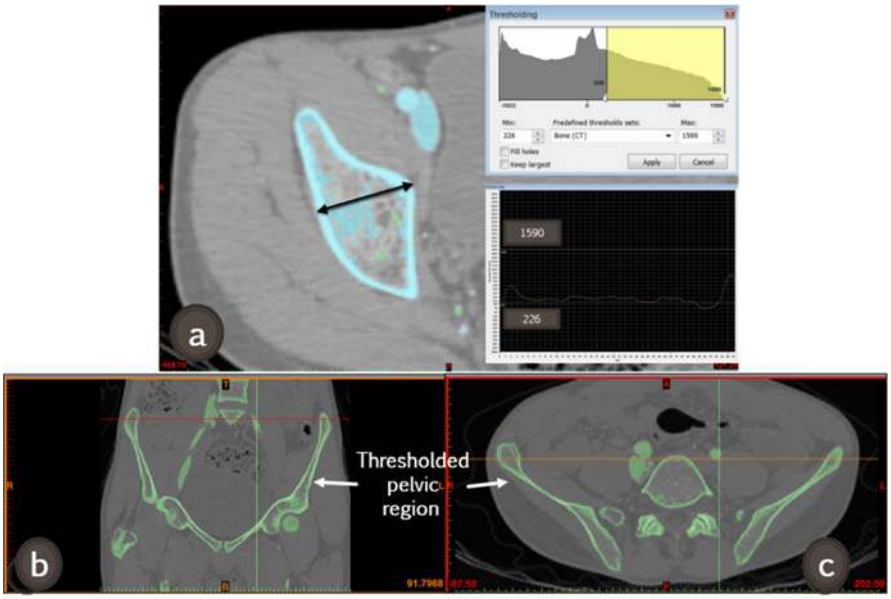

Figure 4.19: CT scan images of lower limb are thresholded with Bone (CT) scale. (a) Frontal view (b) Tansversal view of thresholded pelvic bone in a green mask

Region Grow:

This tool is used to enhance the region of interest that is the pelvic bone, in order to separate the bone geometry from CT scan. 6-connectivity is used instead of 26-connectivity so as to avoid the nodes and vertices of the selected voxel and include only the neighboring faces of the selected voxel. All points that are connected to the marked point in the current segmentation object will be moved to the target mask.

The arteries, veins and osseous structures were easily distinguished and consequently rendered with red, blue and light grayish orange mask (Figure 1A). The common iliac vein and their associated branches that were adjacent to, and posterior to the arteries contained no contrast medium, so they were not identifiable (except external iliac vein).

Manual segmentation:

This is essentially performed on each slice after region growing so that the resulting left out pixels are also involved in the region grown mask. This is done manually by using draw tool in edit mask. Also, the unwanted connected pixels can be deleted by using erase tool. This is a rigorous and time consuming process as each slice of the CT data is to be keenly observed to preserve the exact boundary of the geometry for which 3D is to be calculated (Figure 4.20). The edit mask tool under segmentation helps to perform draw, erase or local threshold operations on each individual slice for each mask.

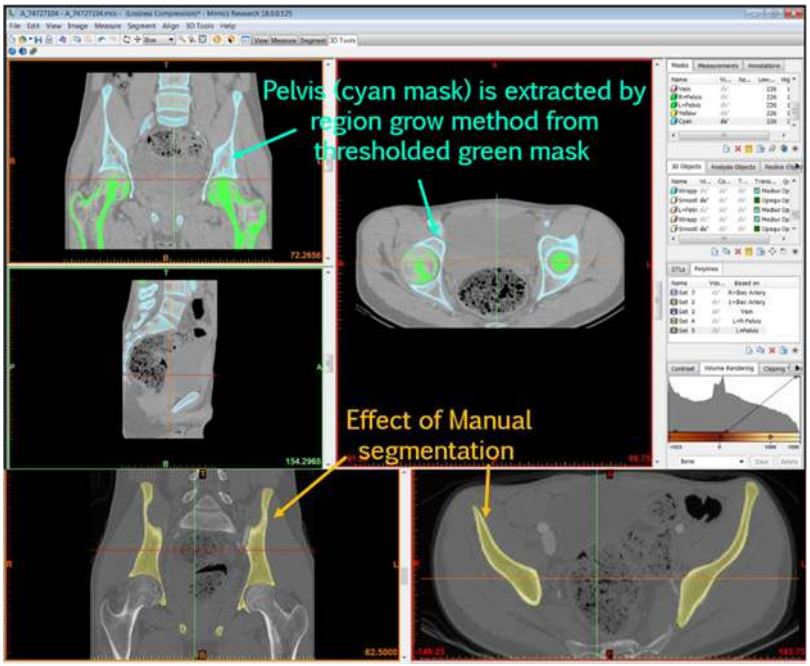

Figure 4.20: Investigation of each scanned slice using Region Grow followed by manual segmentation to develop accurate 3D model

A complete segmentation (including partial automatic segmentation followed by manual segmentation) of pelvis along with arteries and veins (Figure 4.20) was performed in the study.

Smoothing:

This is performed to filter the unwanted pixels resulting from manual segmentation, there by preserving important boundaries. It helps in the removal of artifacts present in the mask and subsequently improves the quality of the developed 3D objects. A smooth mask operation was performed with a smooth factor: 0.5 and no. of iterations: 3.

Calculate 3D:

Here the created masks with the lower and higher threshold mentioned are listed. We selected the desired mask from which 3D volume was to be created (Figure 4.21). An optimal quality was selected to convert the region grown mask into a 3D volume. Finally, 3D model was calculated for each of the red, blue and greyish orange mask for artery, veins and pelvic bone, respectively as shown in figure 4.22.

Figure 4.21: Data conversion from 2D CT images to 3 D model using Mimics Software

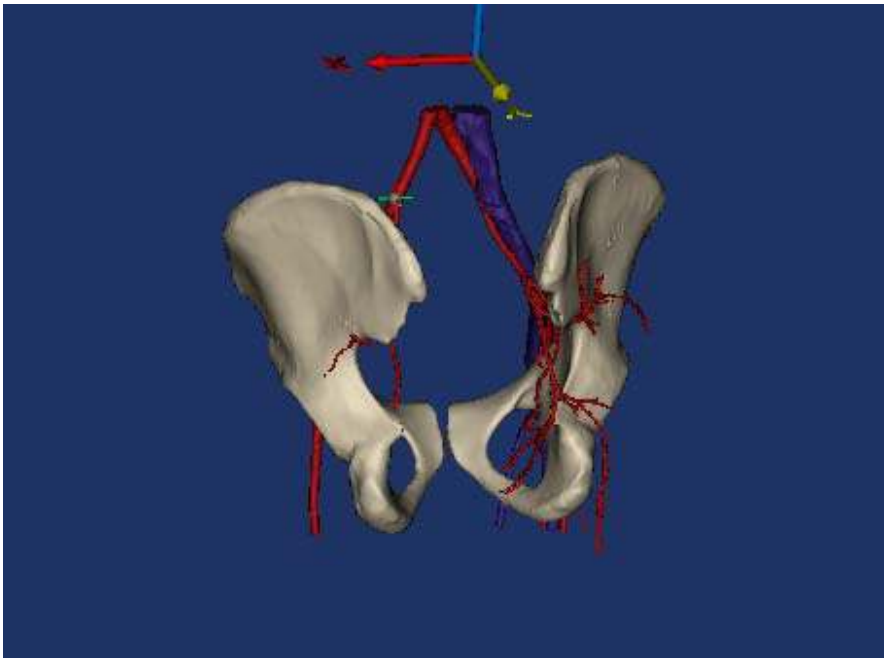

Figure 4.22: Developed 3D model of pelvis and its associated neuro-vascular structure

We modelled the volumetric data of thirty-eight hips into three-dimensional images based on CT.

4.10 3D-Model optimization & modification

The developed 3D pelvis model in Mimics is imported in 3-matic Medical 9.0 software in order to optimize its geometry, create surface mesh and volume mesh. 3-matic is a unique software that combines CAD tools with pre-processing (meshing) capabilities. Surface meshing followed by volume meshing was performed here. Each artery, vein as well as pelvis was fixed by running the fix wizard tool under fix option in order to optimize the surface and volume mesh and modify the surface and volume of the developed 3D geometry. Each of the three masks namely Red, Blue and Greyish Orange rendered for arteries, veins and pelvis were exported directly from Mimics to 3-matic (figure 4.23).

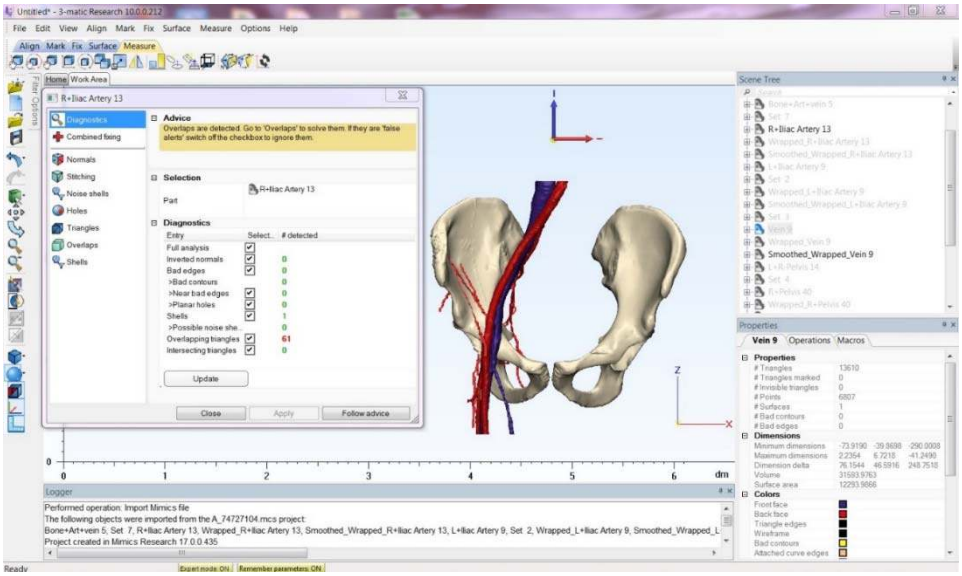

Figure 4.23: Model optimization in 3-matic Medical 9.0

Local smoothing was performed on the rough surface of pelvic geometry and the effect is clearly shown in figure 4.24.

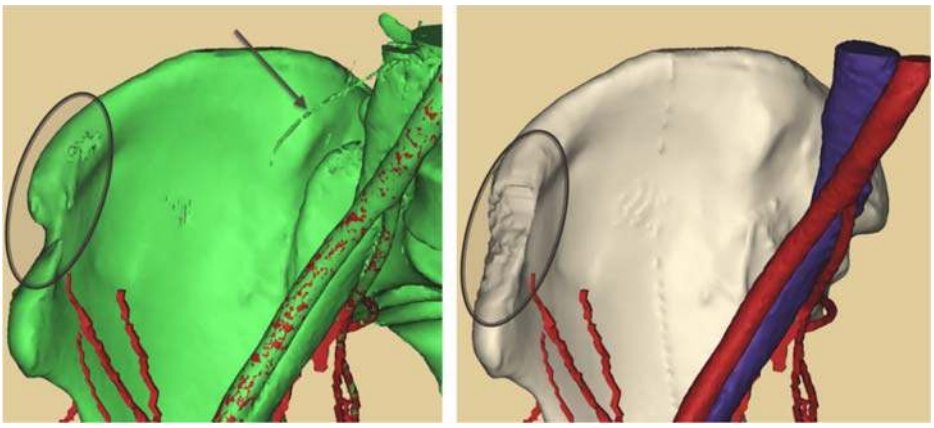

Figure 4.24: Effect of applying local smoothing on developed 3D pelvis model

Remeshing is done to optimize your models for FEA (Finite Element Analysis) purposes. It allows to easily and quickly convert bad shaped triangles to proper equilateral triangles. The more accurate results will be obtained for FEA calculations if the triangles have a more regular geometry.

4.10.1 Inspecting Element quality

The element types that are used in 3-matic Medical are triangle surface elements and tetrahedral volume elements. The quality of the mesh is assessed by how well the elements resemble equilateral triangles and tetrahedrons. This quality influences the capability of the solver program to converge to a solution and affects the accuracy of the numerical simulation. Sharp angles, flat angles or a distorted shape are typical indications for a bad quality element.

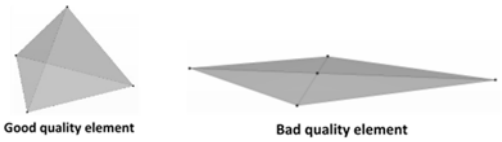

Figure 4.25: Geometry illustrating the difference between good and bad quality elements used for meshing

The quality of the elements can be inspected with shape measures related to triangle properties such as base, length, angle, height, etc. These shape measures indicate how much the elements resemble an equilateral triangle or tetrahedral element.

4.10.2 Typical remesh workflow

The process used to attain a remeshed model in 3-matic is shown in figure 4.26 and each step is described below.

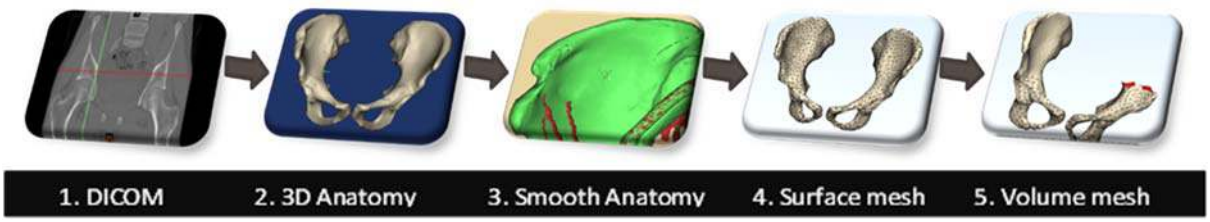

Figure 4.26: Typical workflow of model optimization in 3-matic Medical

1. *DICOM (Mimics Medical)*

Mimics Medical allows you to segment the anatomy of interest from DICOM images.

2. *3D anatomy (Mimics Medical)*

From the segmented DICOM images a 3D part can be generated, which can be exported to 3-matic Medical for further pre-processing.

3. *Smooth anatomy (3-matic Medical)*

Often parts contain little details/artefacts that are not needed for the final FEA/CFD simulation. Representing these details requires a small triangulation, which increases the total number of nodes. By performing the *Smooth* or *Wrap* operations, the geometry & topology of the part can be simplified. This reduces the total number of triangles needed to represent the part.

4. *Optimized mesh (3-matic Medical)*

3-matic Medical contains several tools to optimize the surface element quality:

- Adaptive Remesh: Optimize and locally refine the mesh while preserving detailed features.
- Uniform Remesh: Provides a uniform and high quality surface mesh.
- Gradient Remesh: Improve the growth rate between the elements.
- Quality Preserving Reduce Triangles: Reduce triangles while preserving element quality.

Once you are satisfied with the surface mesh, the “Create Volume Mesh” tool will generate tetrahedral elements starting from the surface elements.

4.10.3 Volume meshing

A volume mesh is necessary for FEA purpose. A volume mesh consists of tet-4 or tet-10 elements. Creating Volume Mesh operations helps to quickly create a volume mesh from a surface mesh. The more regular geometry of the triangles for tetrahedrals ensures more reliable and better results of the FEA calculations.

It is also possible to analyze the surface and volume mesh, convert a tet-4 to a tet-10 volume mesh or vice versa and extract a surface mesh from a volume mesh.

Remeshing:

Auto remesh tool was used to perform surface meshing. Surface meshing was performed with shape quality threshold of 0.3, maximum geometrical error of 0.1 and maximum triangle edge length of 1. Accordingly, volume mesh was generated by using create volume mesh tool with maximum edge length of 1 as shown in figure 4.27.

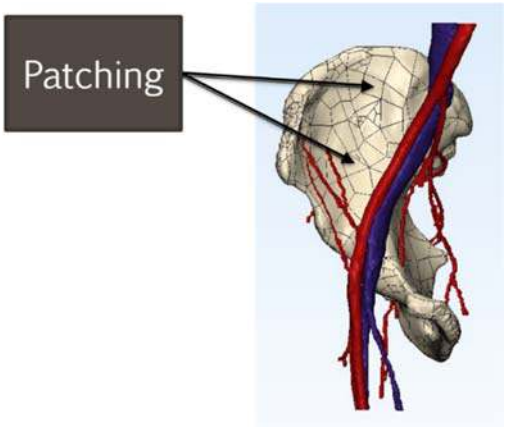

Figure 4.27: Schematic showing the 3D model with remesh parameters

Diagnostics was performed by using fix wizard tool to completely analyze each part. Results were satisfactory with no occurrence or intersecting triangles, possible noise shells or holes.

4.11 Design and assembly of THA components

Development of CAD model of Total Hip Implants & screws as well as surgical simulation of total hip implants with pelvis is performed in CAD software PTC CREO Parametric 3.0 (Student Version) as shown in figure 4.28. Creo Parametric is a 3D Computer Aided Design software for parametric featured modeling based on solid modeling.

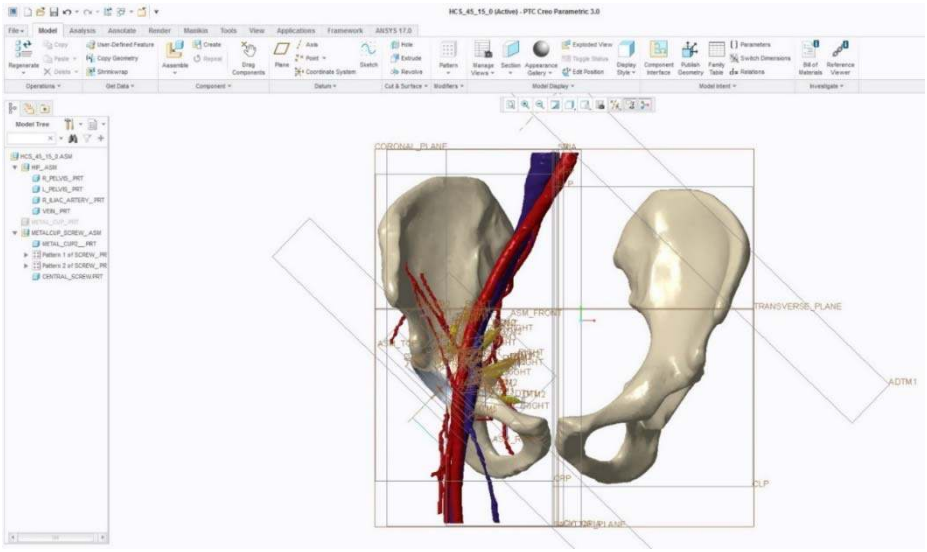

Figure 4.28: Assembly of acetabular cup with twelve screws on pelvis

Creo Parametric 3.0 software (PTC, Inc., Massachusetts, USA) was used to create the 3D model of a proper sized acetabular cup, and the design of a commercially accessible acetabular cup containing 12 screw holes (Pinnacle, Depuy, Warsaw, IN, USA) was used as a template.

However, to mimic 3D screws, the parameters such as screw length, inner diameter, outer diameter, thread length, screw tip are taken into consideration. For our study, these parameters were obtained as discussed below.

4.11.1 Cup and screw design

Cup design is a common parameter to consider when assessing potential success of total hip replacements. FE analysis is a useful tool for pre-clinical analysis of new cup designs, as a direct comparison can be made between the predicted performances of one cup compared to another.

Types of implant

The main ways in which different implants vary are the materials from which they are made and the way that they connect to the existing bone. Only acetabular components will be discussed in this report. There are two main categories of acetabular cup: cemented and press-fit, but a conservative estimate suggests that there are over 80 variations on the market (Havelin et al., 2000).

Cemented cup

In a cemented cup, polymethyl methacrylate (PMMA) bone cement is used to secure a cup into the acetabulum after it has been reamed to the correct size by the surgeon. The cement can act as a load distributer and is compliant enough to absorb some movement. The most common configuration for a cemented cup is an ultra-high molecular weight polyethylene (UHMWPE) cup, but metal backed cups with an UHMWPE or ceramic liner are also used. The stiffness and wear resistance of UHMWPE is much lower than metal or ceramic; this leads to a much thicker cup wall. The thickness of the UHMWPE results in a replacement femoral head which is a lot smaller than the natural bone.

Press-fit cup

An alternative to bone cement is a press-fit cup. These cups have no cement interface, thus the bone grows directly onto the back of the cup. Press-fit cups are predominantly

either all metal, or metal backed with ceramic or polyethylene liner. A cup greater than that of the reamed acetabulum is forced in the bone and thus is constrained in place through pre-stressing the bone. A number of methods are available for encouraging fixation at the cup/bone interface, such as osteoinductive Hydroxyapatite (HA) coating which stimulates bone growth or osteoconductive porous beads which provide a roughened surface onto which bone can grow (Albrektsson and Johansson, 2001). An all metal press-fit cup has fewer interfaces than a cemented cup, but initial fixation is generally more difficult. The lack of cement mantle allows a large femoral head to be used, more representative of the actual femoral head size, and also allowing a large range of motion. Press-fit cups can form part of a standard THR, or a hip resurfacing, in which the minimal amount of femoral head is cut and replaced by a resurfacing head.

Bearing surfaces

The combinations of cup-head bearing surfaces on the market are: metal on UHMWPE; metal on metal; metal on ceramic; ceramic on UHMWPE and ceramic on ceramic. Tribologically, it is preferential to have differential hardness at the bearing surface and to choose a sacrificial part of the bearing couple - that most easily replaced (Medley, 2008). Unfortunately, neither of the implant components can be considered easy to replace, and wear particles are undesirable as they have been linked to osteolysis and implant loosening (Howie et al., 2007). This has led to high hardness materials being used on both implants (e.g. metal on metal) and a clearance designed into the bearing couple to entrain fluid and thus provide a layer of fluid lubrication. Bearing couples with UHMWPE acetabular cups tend to wear heavily compared to metal on metal bearings, despite the introduction of highly cross-linked UHMWPE (Williams et al.,

2007; Anissian et al., 1999). These cups are thus primarily implanted into aged patients with short expected life-spans (under 10 years). There is a new bearing material which has been recently introduced to the market. This is Polyether-ether-ketone (PEEK), a ploymer which can be carbon fibre reinforced to provide a low wearing, low stiffness polymer (Green, 2005). PEEK can be short-fibre reinforced with varying amounts of fibres, allowing a range of stiffness values to be achieved.

The design of a commercially designed acetabular cup having 12 screw holes (Pinnacle, Depuy, Warsaw, IN, USA) was used as a template. The eccentric screw was designed with a length of 25mm, thread length of 0.38 mm as well as inner and outer diameter of 4mm and 5mm, respectively. The design templates for acetabular cups with eccentric holes and eccentric screws are shown in figure 4.29.

The cup must therefore be thin walled and able to accommodate the large femoral head bearing. Subtle differences in cup geometry (such as relative curvature and cup-head clearances) have not been included in this study. This is because the bearing surface geometry governs fluid film lubrication, which is not included in detail in the FE model (it is represented by free sliding at the cup-head interface) and therefore the tribological impact of such changes would not be captured.

We created thirteen standard screws and assembled them in each cup hole of all 38 hips using simulated screw fixations with ideal (screw fixed perpendicular to cup surface) and angular eccentric profiles as illustrated below.

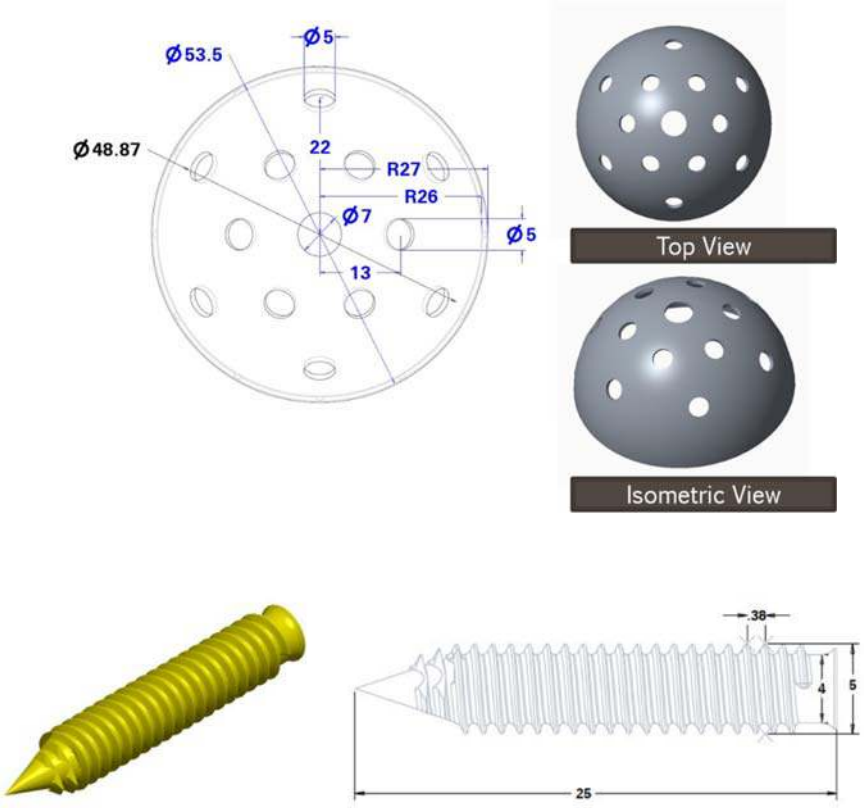

Figure 4.29: 2D Sketches converted to 3D model: above is the draft view of acetabular cup and below is the schematic screw

4.11.2 Angular eccentric screw configuration profiles

The Screw configuration profiles (SCP) are configured and listed in Table 4.2 and demonstrated for all possible angular eccentricity from the manufacturer guideline.

Each cup was simulated with twelve screws and one polar screw. Further, each screw was rotated in accordance with developed SCP as shown in Table 4.2.

4.11.3 Planes and axis of acetabular cup

Two planes are drawn on the pelvic geometry in Creo parametric. The planes are aligned according to the cup inclination and anteversion angles. A blue colored plane shown in the figure is named as Acetabular Plane (AP) and a grey colored plane drawn

perpendicular to AP is named as Acetabular Axis Plane (AXP). At the center of acetabular cup, a black circle is drawn and named as Geometric Centre of Acetabular Cup. A line originating from geometric center of acetabular cup, is drawn perpendicular to acetabular plane (AP), and is termed as Acetabular Axis (AA). All the planes and axis are clearly visible in the figure 4.30.

Screw configuration profile (SCP)	Cup inclination angle (Degree)	Cup anteversion angle (Degree)	Screw angular eccentricity (Degree)	Eighteen developed angular eccentric screw configuration profile (SCP)
SCP-1	45°	15°	0°	SCP-1 (45-15-0)
		20°	0°	SCP-1 (45-20-0)
SCP-2	45°	15°	17°	SCP-2 (45-15-17)
			34°	SCP-2 (45-15-34)
		20°	17°	SCP-2 (45-20-17)
			34°	SCP-2 (45-20-34)
SCP-3	45°	15°	17°	SCP-3 (45-15-17)
			34°	SCP-3 (45-15-34)
		20°	17°	SCP-3 (45-20-17)
			34°	SCP-3 (45-20-34)
SCP-4	45°	15°	17°	SCP-4 (45-15-17)
			34°	SCP-4 (45-15-34)
		20°	17°	SCP-4 (45-20-17)
			34°	SCP-4 (45-20-34)
SCP-5	45°	15°	17°	SCP-5 (45-15-17)
			34°	SCP-5 (45-15-34)
		20°	17°	SCP-5 (45-20-17)
			34°	SCP-5 (45-20-34)

Table 4.2: Set of angular eccentric screw configuration profiles

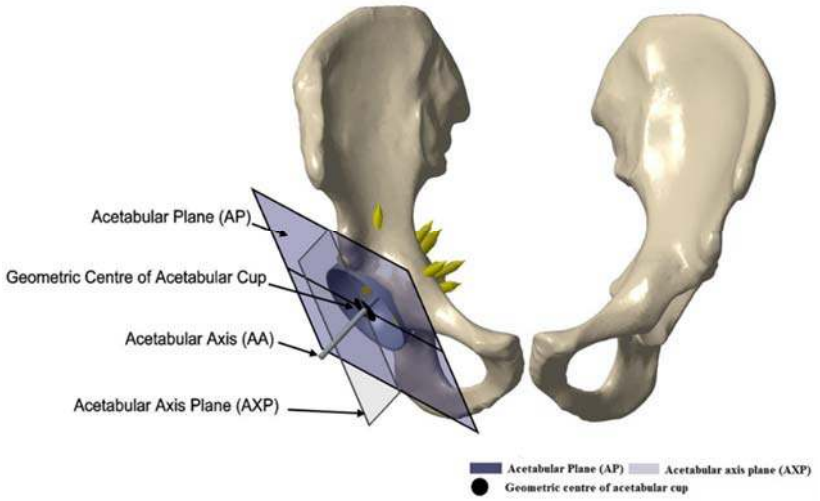

Figure 4.30: Illustration of the planes and axis for placement of acetabular cup.

4.12 Surgical simulation and measurements

Both, the acetabular cup as well as the screws are virtually fixed on the reamed pelvis region. The surgical simulation of THA performed in the study is discussed below. We developed the screw configuration profiles for eccentric screw fixation and proposed criteria to calculate the risk factor of vessels. The corresponding figures clearly depict the complete procedure of virtual fixation of cup and screw according to the screw configuration profile in this chapter. Virtual planes and axis for sup fixation as well as the development of quadrants is also described in the sections below.

4.12.1 Implant orientation

The orientation of the acetabular cup implant is discussed appropriately in this thesis. The position of the cup rim in space is commonly reported through two angles; inclination and version. Cup inclination is defined as the angle in the middle of rim of acetabular cup and the transverse/axial plane (a plane horizontal through the acetabulum bisecting the superior and inferior sections). Cup version is defined as the angle present

in between the rim of acetabular cup and the sagital plane (a plane horizontal through the acetabulum bisecting the medial and lateral sections).

There have been a range of published studies considering additional fixation mechanisms applied to the rear of the cup. These are primarily screws, spikes and fins, in varying position and quantity. Invariably, the addition of such mechanisms reduces the initial micromotion at the cup-bone interface, thus increasing initial implant stability (Baleani et al., 2001; Perona et al., 1992). Such studies also show that the number and location of extra fixations has an influence on the amount of stability they provide. A number of radically different screw orientations, each with a theoretical benefit over existing implants with respect to one or more failure criteria, were included in the study.

For our study, we consider four input parameters to carry out surgical simulation of acetabular cup. These include: cup inclination, cup version, cup interference, seating of cup.

Cup inclination

Cup inclination angle is the angle of orientation of rim of acetabular cup to that of the transverse plane (a plane horizontal through the acetabulum bisecting the superior and inferior sections). The chosen range should reflect the range of achieved angles in surgery. The ‘safe zone’, introduced by Lewinnek and co-workers (1978) states the inclination angle should be between 30° and 50° in order to avoid dislocation. Whereas, Wasielewski et al. in 1990, used the cup inclination angle of 45 degrees. Since the advent of CT-scanning, accurate measurement of inclination angle has been possible. ‘Real’ inclination is measured in three dimensions, whereas previously angles were estimated from planar radiographs. The errors between ‘real’ and radiograph

measurements have been shown to be very large (up to 15°), especially when large diameter bearings are implanted (Hart et al., 2009). The 'safe zone' may therefore be slightly different to that measured by Lewinnek et al. Despite this, 40±10° is still commonly referred to as the target inclination angle.

A large number of studies exist in the literature which measure the achieved inclination and version angles of acetabular cup implants (Kalteis et al., 2006; Lazovic and Kaib, 2005; Saxler et al., 2004). A comprehensive clinical retrospective study with 105 patients and angles measured with CT-scans was used to inform the variation in inclination angles used in this study (Saxler et al., 2004). It is important that the angles used to inform the choices here were measured in the same manner (via CT) as will be implemented in this study.

The inclination angle that was chosen for inclusion was oriented at 45° of inclination.

Cup version

The version angle of the acetabular cup is measured between the rim of the cup and the sagittal plane (a plane vertical through the acetabulum bisecting the medial and lateral sections). Lewinnek's safe zone for version is 5 to 25°. Whereas, Wasielewski et al used the cup anteversion angle of 15 degrees. The sensitivity of version to measurement technique is higher than inclination angle, with plane radiograph measurements underestimating version by up to 31° (Hart et al., 2009a). The same study (Saxler et al., 2004) as was used to estimate the range of inclination angles was used to approximate the range of achieved version angles.

The two version angles chosen for inclusion in the study were: 15° and 20°.

Cup interference

The cementless acetabular cup is press-fitted into an acetabulum reamed to a size smaller than the cup to ensure initial cup stability. Again, an effort was made to include a range of cup interference levels representative of the surgical situation. Cup interference is the diametrical difference in size between the reamed cavity and the implanted cup. The larger the interference the more stable the cup; although interferences higher than 2mm may potentially cause fracture of the underlying bone (Curtis et al., 1992). Depending on the quality of substrate, diametrical interferences of either 1 or 2mm have been shown to provide optimal stability (Adler et al., 1992).

To achieve interference rim fit in reamed acetabulum in our study, the inferior edge of acetabular cup was positioned at a level of bottom of teardrop line together with cup constraining in both posterior and anterior columns in transverse plane.

Seating of cup

Ideally the cup implant should be fully seated inside the reamed acetabulum, to enable bone in-growth over the whole surface. The potential seating of the cup within the reamed acetabulum is dependent on the impaction and frictional coefficient between cup and pelvis. Press-fit cups have been shown experimentally to be in contact predominantly around the rim of the cup, and not at the dome (Kim et al., 1995a; Mackenzie et al., 1994). The experimentally observed gaps between the dome of the cup and the base of the acetabulum increased with radial size of the acetabulum and averaged 2.7mm (SD 1.1) when an interference fit of 1mm was present, and 3.1mm (SD 1.1) when an interference fit of 2 mm was present (Kim et al., 1995a). The cups included

in the study had a diameter of 53.5 mm with polar screw of diameter 7 mm and eccentric holes of diameter 5 mm.

4.12.2 Surgical simulation of acetabular cup: Cup fixation

For simulating clinical surgery, acetabular position is fitted in orthographic sagittal and coronal planes at a level of true acetabulum and is inclined at 45° with anteversion angle of 15° and 20° (Figure 4.31).

The cup is aligned to Acetabular Plane (AP) and Acetabular Axis Plane (AXP). The center of acetabular cup is aligned to the Geometric center of acetabular cup and the Acetabular Axis (AA) in order attach the cup appropriately to the pelvis. To achieve interference rim fit in reamed acetabulum, we positioned the inferior edge of the cup at the level of the bottom of teardrop line together with cup constraining in both anterior and posterior columns in the transverse plane.

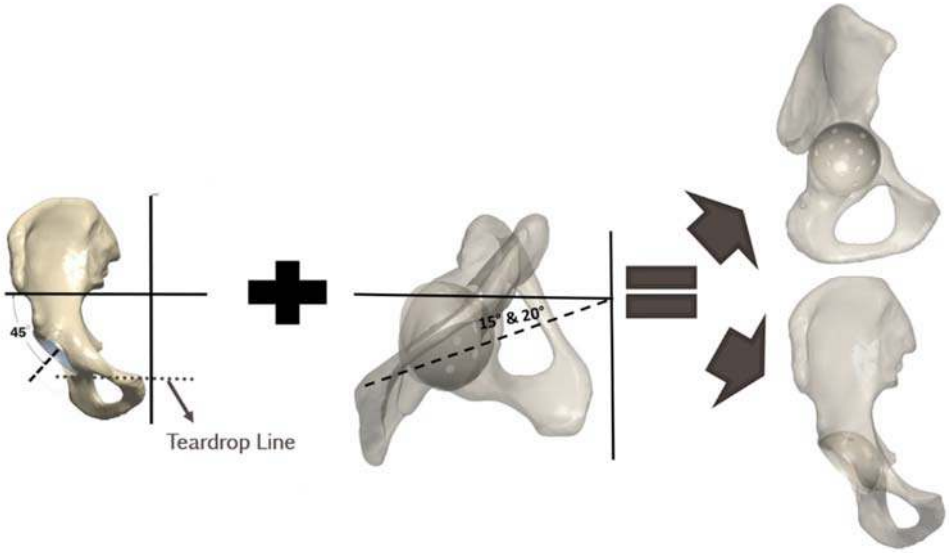

Figure 4.31: Schematic representing the cup inclination, cup version angles as well as cup interference for fixation of the cementless pressfit cup into the pelvis

4.12.3 Surgical simulation of eccentric screw: Screw fixation

Screws are fixed perpendicular to the cup surface. This is the ideal fixation (Figure 4.32). However, screws are fixed on the eccentric holes according to different Screw Configuration Profiles (SCP).

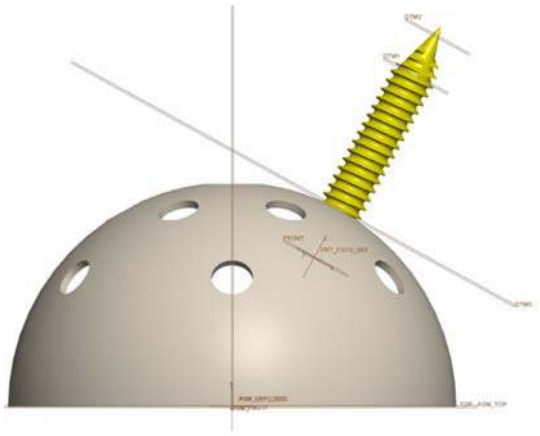

Figure 4.32: Assembly of eccentric screw on the acetabular cup with eccentric holes

Fixation of all twelve screws were performed according to their SCP (Figure 4.33-4.37).

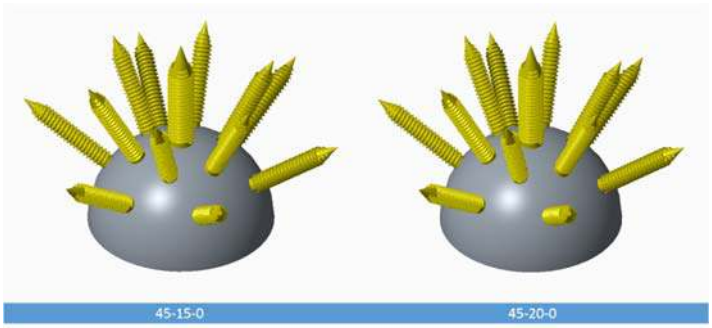

Figure 4.33: Illustration of SCP-1 with screw eccentricity of 0° and cup anteversion angle (a) 15° (b) 20°

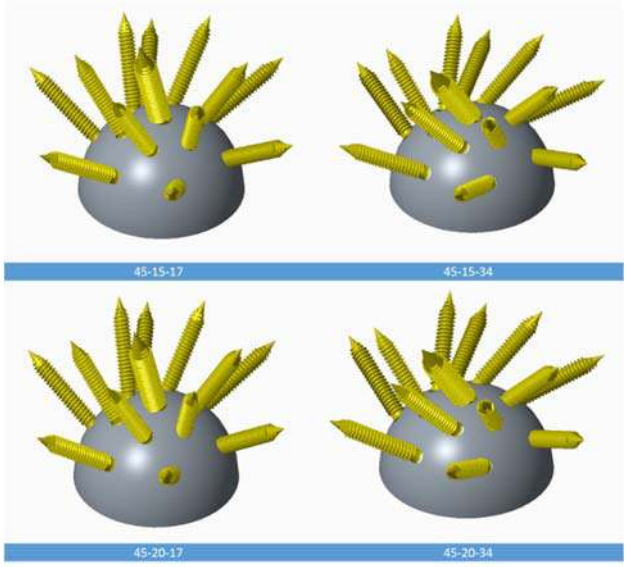

Figure 4.34: SCP-2 containing four profiles. (a) Cup anteversion angle: 15°, screw eccentricity: 17° (b) cup anteversion angle: 15°, screw eccentricity: 34° (c) cup anteversion angle: 20°, screw eccentricity: 17° (d) cup anteversion angle: 20°, screw eccentricity: 34°

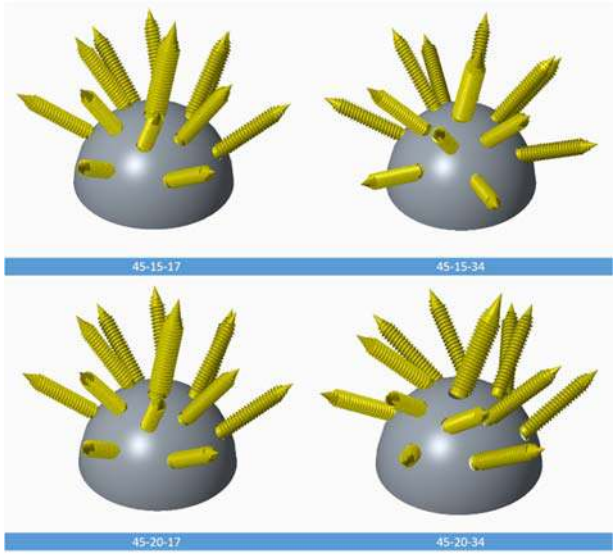

Figure 4.35: SCP-3 containing four profiles. (a) Cup anteversion angle: 15°, screw eccentricity: 17° (b) cup anteversion angle: 15°, screw eccentricity: 34° (c) cup anteversion angle: 20°, screw eccentricity: 17° (d) cup anteversion angle: 20°, screw eccentricity: 34°

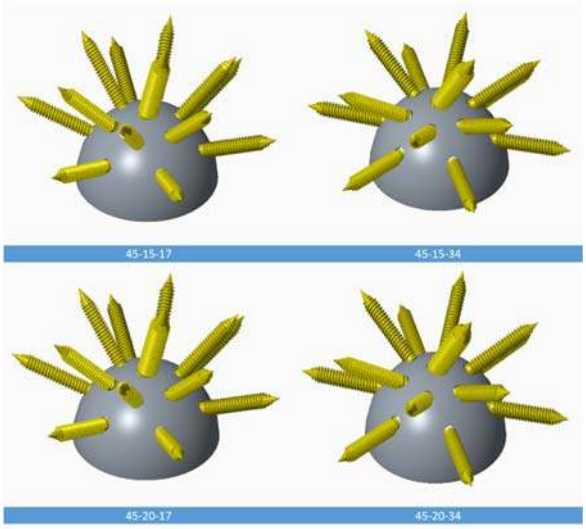

Figure 4.36: SCP-4 containing four profiles. (a) Cup anteversion angle: 15°, screw eccentricity: 17° (b) cup anteversion angle: 15°, screw eccentricity: 34° (c) cup anteversion angle: 20°, screw eccentricity: 17° (d) cup anteversion angle: 20°, screw eccentricity: 34°

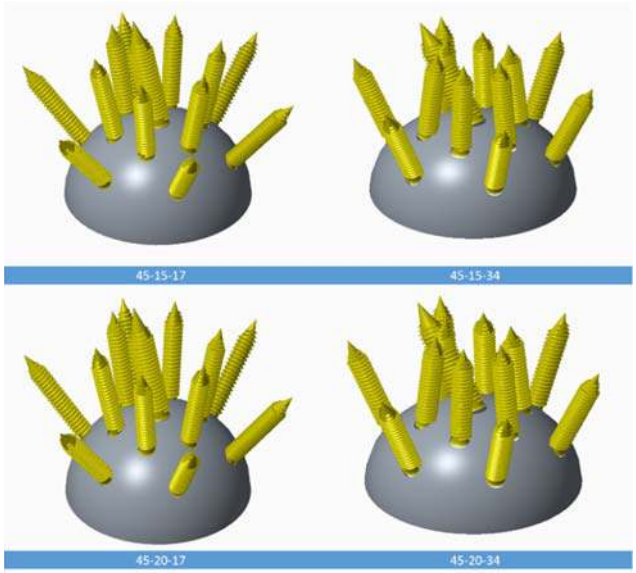

Figure 4.37: SCP-2 containing four profiles. (a) Cup anteversion angle: 15°, screw eccentricity: 17° (b) cup anteversion angle: 15°, screw eccentricity: 34° (c) cup anteversion angle: 20°, screw eccentricity: 17° (d) cup anteversion angle: 20°, screw eccentricity: 34°

Whereas for polar screw, fixations were made along with subsequent SCP (1-5) as shown in Figure 4.38 (A-F), but it is quiet not imaginative in figure so described below as:

SCP-1 In Ideal Screw fixation, polar screw's axis was lying on the fixed acetabular axis (AA) passing through the geometric center of the acetabular cup (Figure 4.38A).

SCP-2 For polar screw, angular eccentricity is along acetabular axis plane (AXP), towards acetabular plane (AP) inferiorly (Figure 4.38F).

SCP-3 For a polar screw, angular eccentricity is along acetabular axis plane (AXP), towards acetabular plane (AP) superiorly (Figure 4.38F).

SCP-4 For a polar screw, angular eccentricity is along the plane perpendicular to acetabular axis plane (AXP) and towards acetabular plane (AP) posteriorly (Figure 4.38F).

SCP-5 For a polar screw, angular eccentricity is along the plane perpendicular to acetabular axis plane (AXP) and towards acetabular plane (AP) anteriorly (Figure 4.38F).

Semi-transparent screw in figure B, C, D, E and F shows the ideal screw fixation and angular arrows are outlined as the screw rotation on specified plane. 17° and 34° rotation contemplated for every screw configuration profiles (SCP) independently. In figure F, polar screw configuration is demonstrated which is associated with SCP-2, SCP-3, SCP-4, SCP-5 consequently. Abbreviation: SCP= Screw configuration profile, AP=Acetabular plane, AXP=Acetabular axis plane, ⊥AXP= Plane perpendicular to acetabular axis plane (AXP).

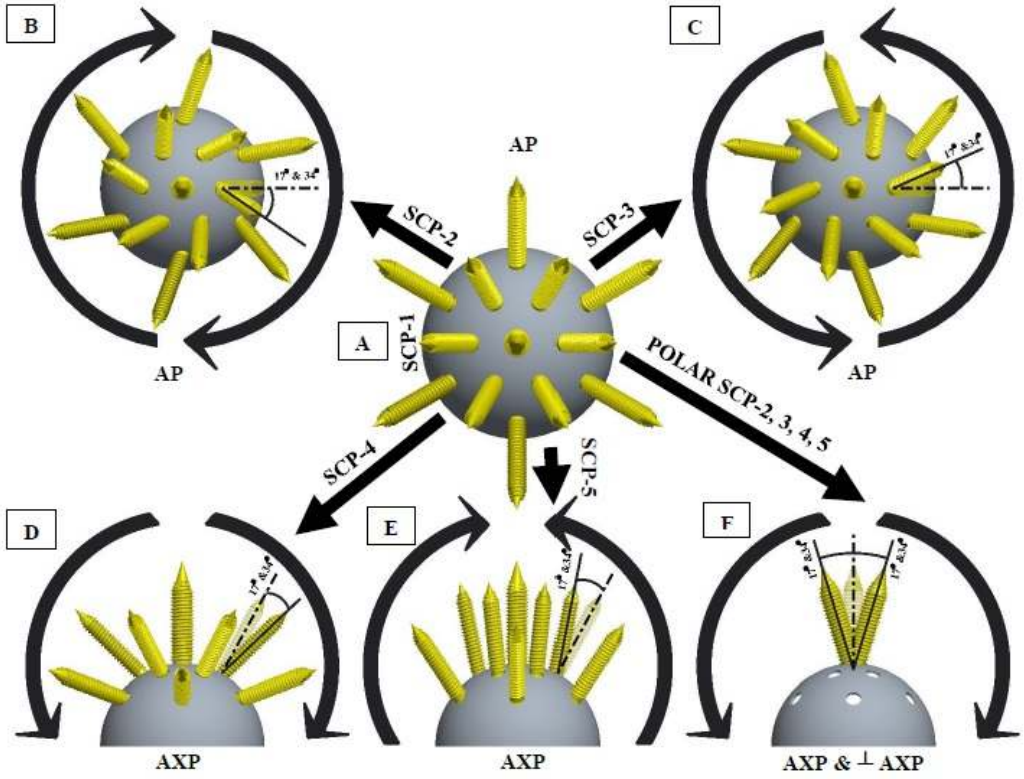

Figure 4.38: (A-F). The ideal fixation and angular eccentric fixation of screws.

4.13 Development of quadrant system Using a simple quadrant system for acetabulum proposed by Wasielewski et al., we divided acetabular cup using two perpendicular lines. The first line A, joining the anterosuperior iliac spine (ASIS) with the acetabulum center, results in two halves of an anterior and posterior region. The

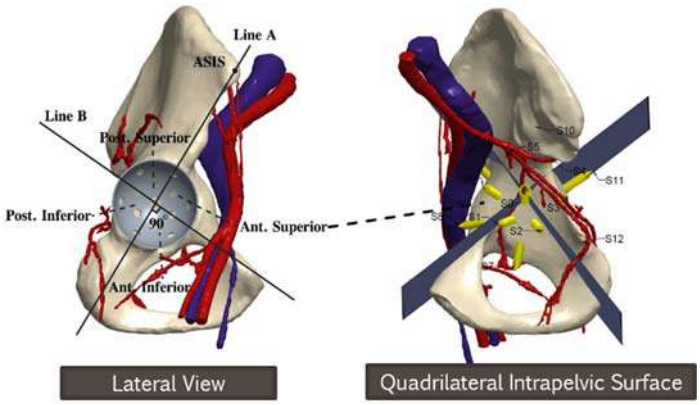

Figure 4.39: 3D computational model of osseous and arterial structures. Schematic diagram illustrating the quadrant system proposed by Wasielewski et al.

second line B, perpendicular to the first line (line A) also passed through the center of the acetabulum to create superior and inferior hemi-quadrants (Figure 1A).

4.14 Calculating the risk on vascular structures due to positioning of eccentric screws

To consider the risk of injury to vessels, it is essential to calculate the risk factor associated with the placement of each screw for each configured Screw Configuration Profile included in the study. Therefore, we developed a set of four criteria for determining the fixation of screws in the developed quadrants and studying the effect of screw eccentricity on the vessels in proximity to the acetabulum.

Table 4.3 enlists all the criteria with its associated risk factors and considerations.

4.14.1 Initial Criteria for consider the risk factor of vessels

C1- Structures were entirely safe if, they were at a distance >20 mm from the screw.

C2- Structures were considered safe, if screw tip was not directed to blood vessels with a distance >5 mm.

C3- Structures were considered at risk, if they felt within 5 mm to 20 mm from the screw.

C4- Structures were considered fully insulted, if they were hit and punctured by the screw, or structures that touched the tip of screw and/or having a distance <5mm.

However, we consider that the screws, which lie inside the bone, are entirely safe and hence, do not fall in the above criteria.

Table 4.3: Set-up of initial criteria to consider the risk factor associated with screw eccentricity

CRITERION	RISK FACTOR	CONSIDERATIONS
C1	**Structures were entirely safe**	**If they were at a distance >20 mm from the screw.**
C2	**Structures were considerably safe**	**if screw tip was not directed to blood vessels with a distance >5 mm.**
C3	**Structures were considered at risk**	**If they felt within 5 mm to 20 mm from the screw and screw tip was directed to blood vessels**
C4	**Structures were considered fully insulted**	**If they were hit and punctured by the screw, or structures that touched the tip of screw and/or having a distance <5mm.**

To estimate the relative risk of different eccentric profiles of the screws on blood vessels proximal to pelvic bones, we used analysis tool in Creo Parametric (student version) at each level to measure the distance between screw and adjoining blood vessel. We then calculated the contiguous mean distance and their standard deviation (SD) from the major blood vessels like obturator artery, external iliac artery, external iliac vein, superior gluteal artery and inferior gluteal artery to its adjacent screws in all 38 subjects.

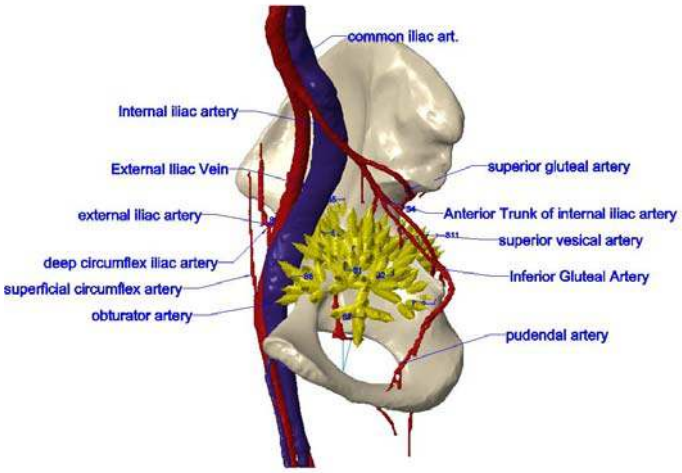

Figure 4.40: Schematic of the intrapelvic bony surface anatomy fitted with acetabular cup and screws.

After placing the screws on the cup, we measure the distance between the screw tip and vascular structure in its vicinity. As a result, we observed that screws S0, S1, S4, S7 and S8 were found closest to obturator artery (Table 4.4). Therefore, we considered only these screws for the analysis. Similarly, for external iliac vein, screws S5, S6, S8 and S9 were observed to be closest and considered in the study (Table 4.4). Screws S5, S6, S8 and S9 were again studied for external iliac artery because of their close proximity to the vessel (Table 4.4). Inferior gluteal artery contained screw S0, S2, S3 and S12 in its vicinity and hence is considered for analysis (Table 4.4). Superior gluteal artery had screws S3 and S12 closest to it and hence were studied for measurement (Table 4.4). A complete measurement study of all the major vessels along with its considered screws was performed and the measured data was used to calculate the mean and standard deviation (SD). The mean and SD for each screw associated with its vessel is tabulated and represented in table 4.4 (next page).

Table 4.4: Table showing distance (mm) and standard deviation (SD) of all 38 patients from vessel structures to their corresponding screw in different SCP

	Screw configuration profile (SCP)																	
	SCP-1 (45-15-0)	SCP-1 (45-20-0)	SCP-2 (45-15-17)	SCP-2 (45-15-34)	SCP-2 (45-20-17)	SCP-2 (45-20-34)	SCP-3 (45-15-17)	SCP-3 (45-15-34)	SCP-3 (45-20-17)	SCP-3 (45-20-34)	SCP-4 (45-15-17)	SCP-4 (45-15-34)	SCP-4 (45-20-17)	SCP-4 (45-20-34)	SCP-5 (45-20-17)	SCP-5 (45-20-34)	SCP-5 (45-20-17)	SCP-5 (45-20-34)
Obturator artery and screw (S0)																		
Mean	0	0	0	5.36	1.75	2.98	0.94	1.04	1.11		0.52	5.63	4.47	12.00	0	0	0	0
SD	0	0	0	0.96	0.65	1.16	0.75	0.78	0.67		0.62	1.23	1.21	1.46	0	0	0	0
Obturator artery and screw (S1)																		
Mean	0	0	0	0	0	0	0.90	3.07	1.70	3.17	0	0	0	0	0	0	0	0
SD	0	0	0	0	0	0	0.67	1.09	0.92	1.18	0	0	0	0	0	0	0	0
Obturator artery and screw (S4)																		
Mean																4.25		7.60
SD																0.88		0.94
Obturator artery and screw (S7)																		
Mean	8.03	11.36	7.59	5.04	12.13	8.08												
SD	1.48	1.24	1.56	1.08	0.84	1.47												
Obturator artery and screw (S8)																		

Mean	16.78						10.04	5.97		8.16					12.49		9.44	9.65
SD	1.61						0.97	0.85		1.07					1.48		1.17	0.74
External iliac vein and screw (S5)																		
Mean	16.97						8.30	5.50	12.21	6.60					16.18	18.27		21.85
SD	1.69						1.04	0.47	0.88	0.65					0.93	1.43		1.16
External iliac vein and screw (S6)																		
Mean	8.95	9.82	2.32	6.00	3.36	9.42	18.96	22.27	16.38	25.87	8.22	0	6.90	0	15.10	16.91	15.05	21.63
SD	1.57	0.77	0.44	0.95	1.01	0.78	1.35	2.05	1.01	2.32	0.84	0	1.06	0	1.40	1.76	0.97	1.32
External iliac vein and screw (S8)																		
Mean	9.38	11.28	10.99	0	4.95	0	15.47	30.31	30.23	20.29	14.29	14.09	16.40	9.16	19.32	11.13	15.41	19.04
SD	1.48	1.01	1.01	0	1.03	0	1.80	0.93	1.00	1.43	1.18	1.04	1.29	1.21	1.32	0.85	1.32	1.33
External iliac vein and screw (S9)																		
Mean	15.53	25.22	19.45	28.93			1.13	0.73	5.75	0	20.95				9.40	4.27	10.49	6.52
SD	1.02	1.35	2.78	1.45			0.59	0.61	1.07	0	0.72				0.93	1.00	0.44	0.53

External iliac artery and screw (S5)																		
Mean	26.33						21.02	14.44	21.81	16.50								
SD	1.37						1.12	0.95	1.65	1.60								
External iliac artery and screw (S6)																		
Mean	19.98	24.43	16.64	21.18	20.17	25.21	25.21	34.97	30.32		15.84	12.76		11.83				

SD	1.18	1.14	1.54	1.25	1.46	0.63	1.23	0.95	0.32		1.30	1.72		1.02				
External iliac artery and screw (S8)																		
Mean	28.45	24.83		10.10	19.56	15.74			44.40		26.76	21.86		16.51	30.88			
SD	1.75	1.10		0.88	0.97	1.21			1.88		1.61	1.30		1.71	1.58			
External iliac artery and screw (S9)																		
Mean	7.99	9.54	19.01	25.77			0.87	1.15	2.07	5.15	14.66				9.15	14.30	14.96	16.49
SD	1.12	1.21	1.18	1.38			0.53	0.70	0.40	0.91	0.74				1.04	1.28	1.25	1.09
Inferior gluteal artery and screw (S0)																		
Mean	9.88	7.48	17.81		15.90				12.15		3.80	0.66	2.77	7.34	18.44		17.26	
SD	1.14	1.05	1.48		1.06				0.99		1.40	0.52	1.26	0.83	1.21		1.48	
Inferior gluteal artery and screw (S2)																		
Mean	21.01	20.11					14.20	7.27	13.07	16.45				14.25	17.13	12.84	16.01	14.46
SD	1.34	0.89					1.37	0.83	1.17	1.42				1.15	1.83	1.50	1.02	1.33
Inferior gluteal artery and screw (S3)																		
Mean	6.16	8.94	2.90	11.72	4.99	11.22	16.38		20.96		11.78	19.92	14.79		2.12	8.27	6.48	8.47
SD	1.10	1.13	1.17	1.29	1.00	1.05	1.18		1.45		1.26	1.29	0.61		0.74	0.41	0.46	0.95
Inferior gluteal artery and screw (S12)																		
Mean			9.35	8.41	11.39	9.80	14.31								8.41	8.36		8.45
SD			1.24	1.12	0.92	1.18	1.20								0.46	0.99		1.07
Superior gluteal artery and screw (S3)																		
Mean	9.32	9.80	6.29	15.53	7.91	12.02	14.35		20.38	28.64	8.97	8.74	9.23	9.13	8.27	13.29	11.30	14.07

SD	1.08	1.24	1.17	0.96	1.28	1.65	1.33		0.69	1.88	1.38	0.59	0.98	1.07	1.29	1.27	0.95	1.27
Superior gluteal artery and screw (S12)																		
Mean							12.47	0.98	8.55	0						12.03		10.85
SD							1.23	0.77	1.04	0						0.78		0.93

4.15 Results

In order to ascertain a comparative risk study of blood vessels that are not visible during surgery, with different SCPs, a relationship was established by measuring the distance between corresponding arteries, veins and all rotated screws according to SCP's (Table 4.4).

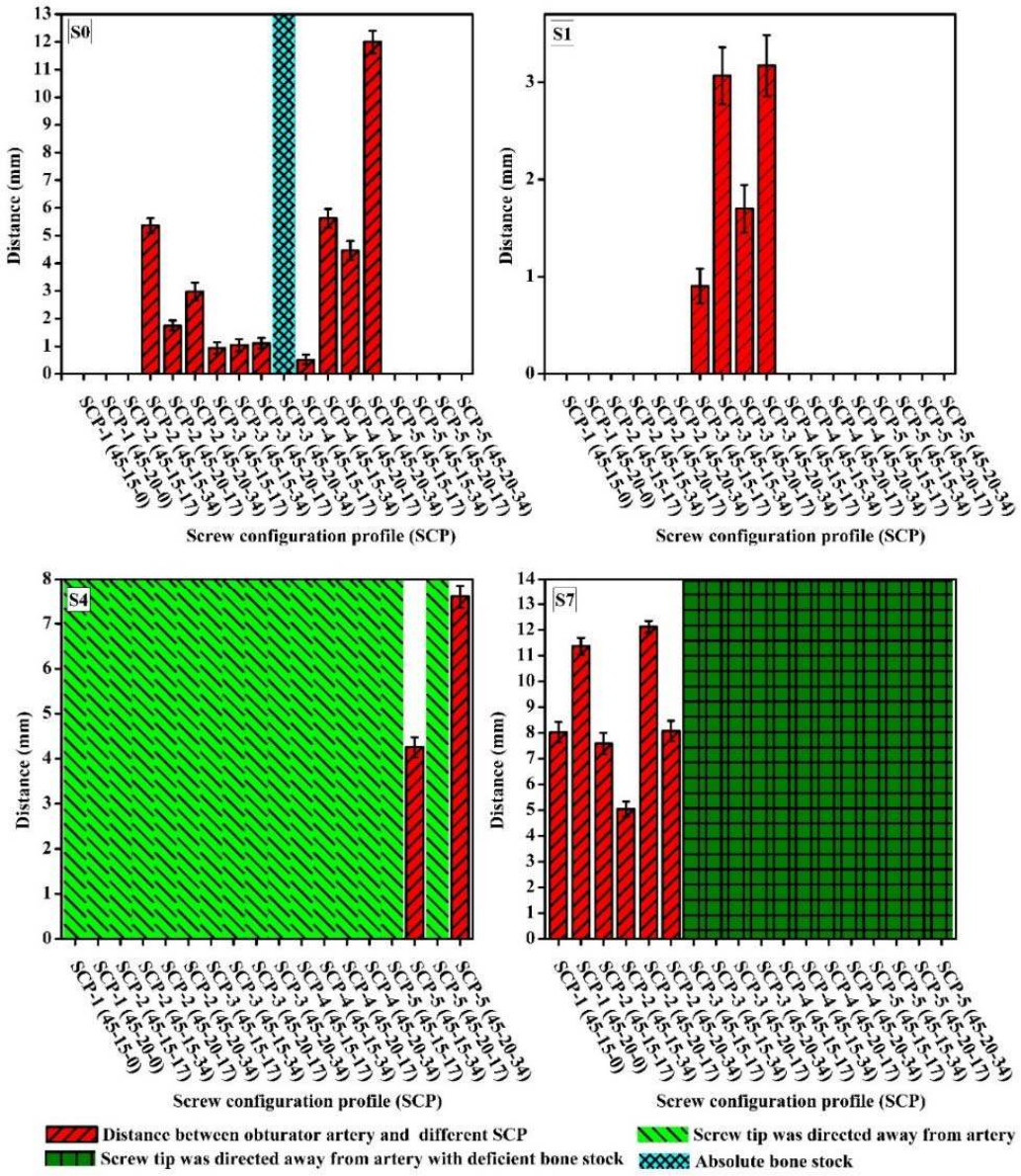

Figure 4.41: Graphs showing the distance measured from screw S0, S1, S4 and S7 to Obturator artery

The tabulated data is graphically represented below in figure 4.41-4.45, which clearly indicates the distance between the vessel and screw for different SCPs. The graphs also show the presence of absolute bone stock and deficient bone stock regions as well as the direction of screw tip which may either be directed towards or away from the vessels.

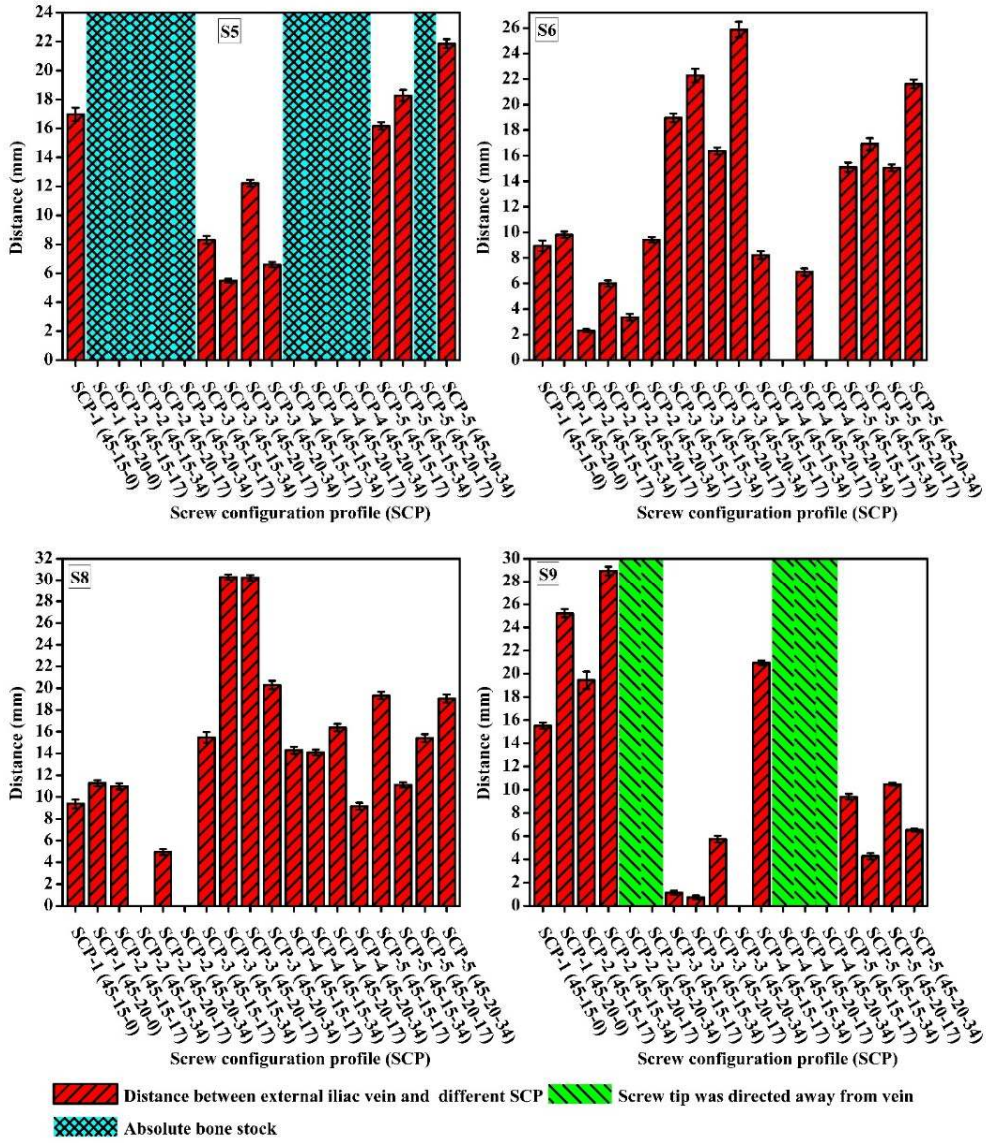

Figure 4.42: Graphs showing the distance measured from screw S5, S6, S8 and S9 to External iliac vein

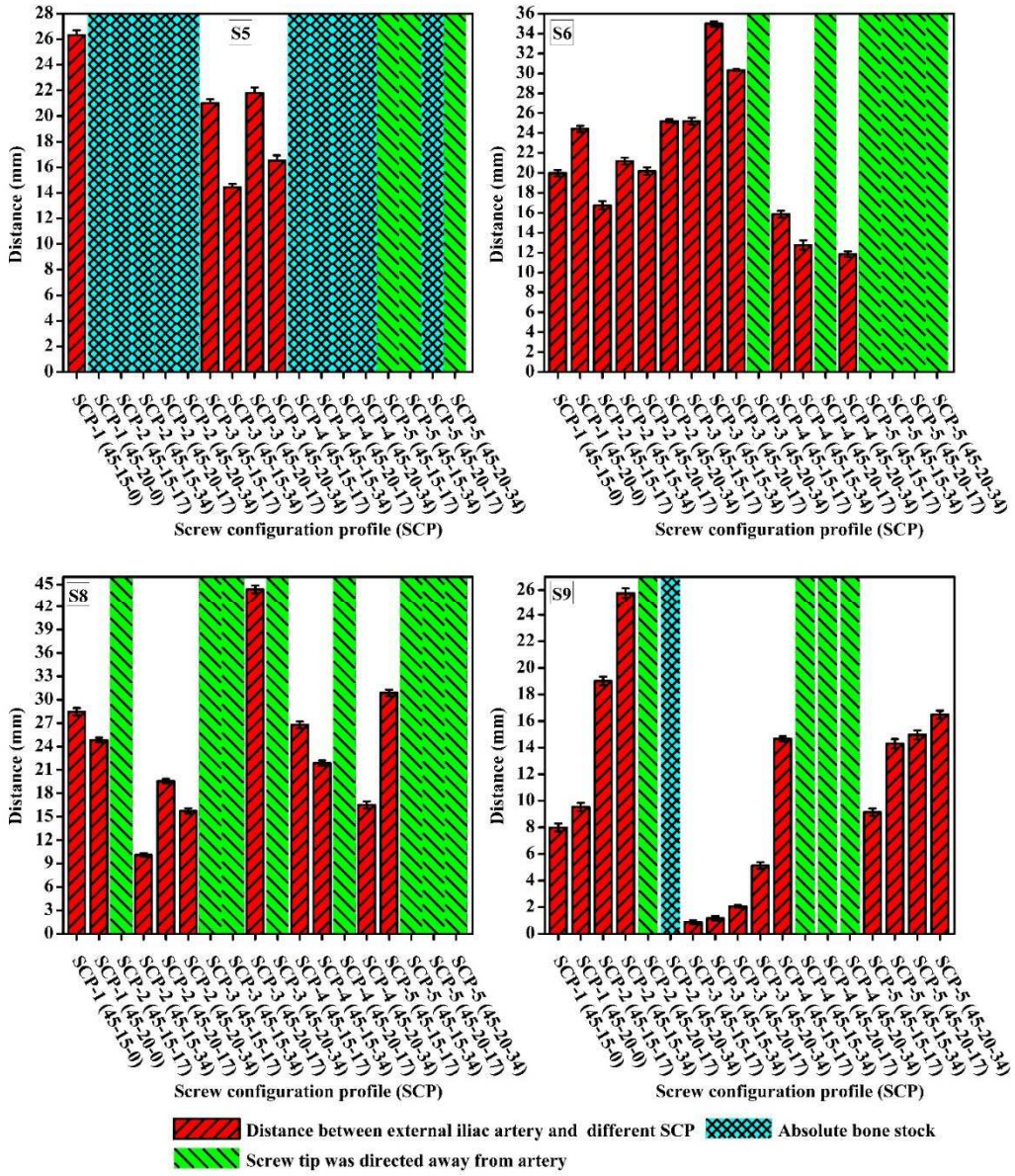

Figure 4.43: Graphs showing the distance measured from screw S5, S6, S8 and S9 to External iliac artery

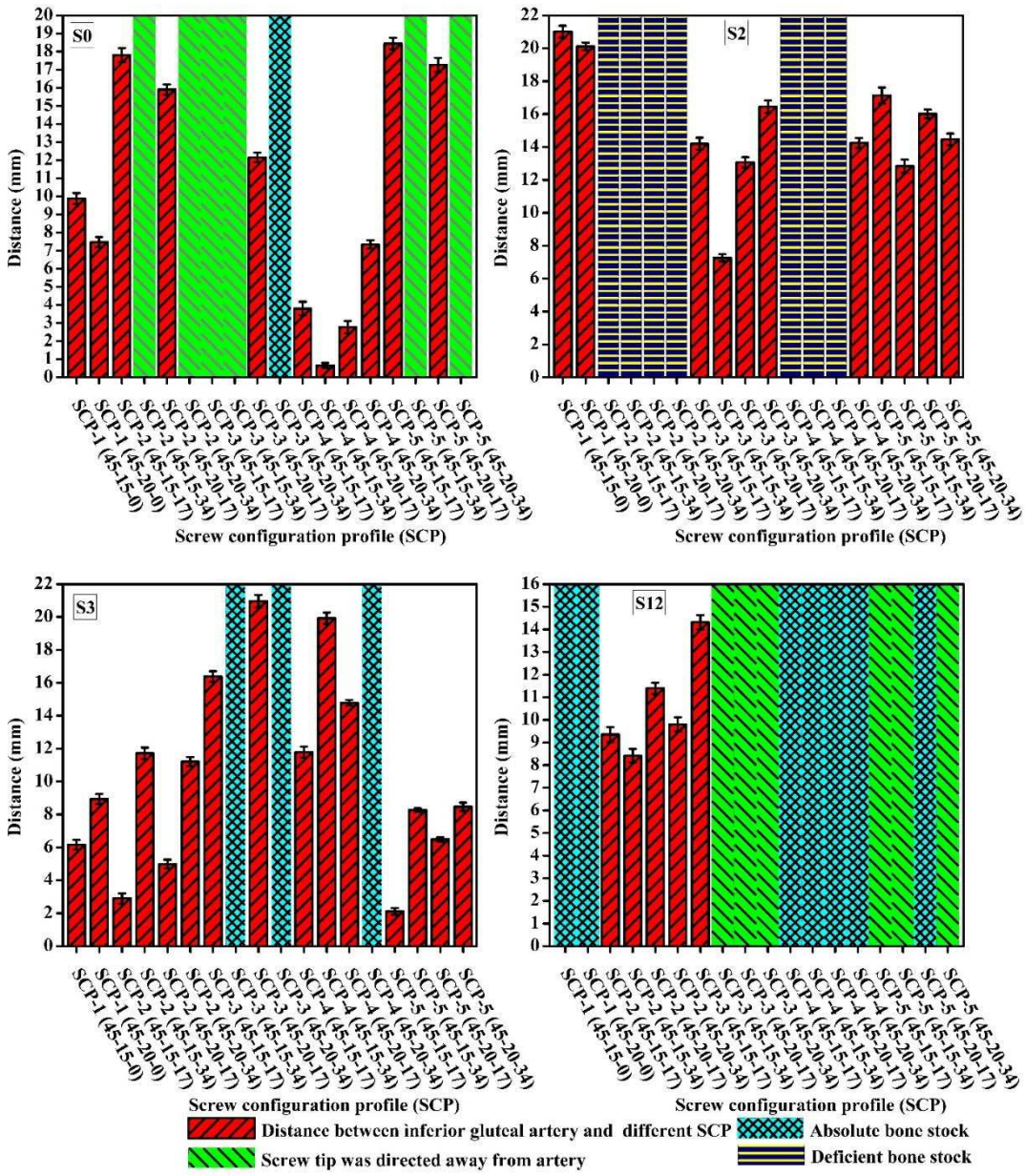

Figure 4.44: Graphs showing the distance measured from screw S0, S2, S3 and S12 to Inferior gluteal artery

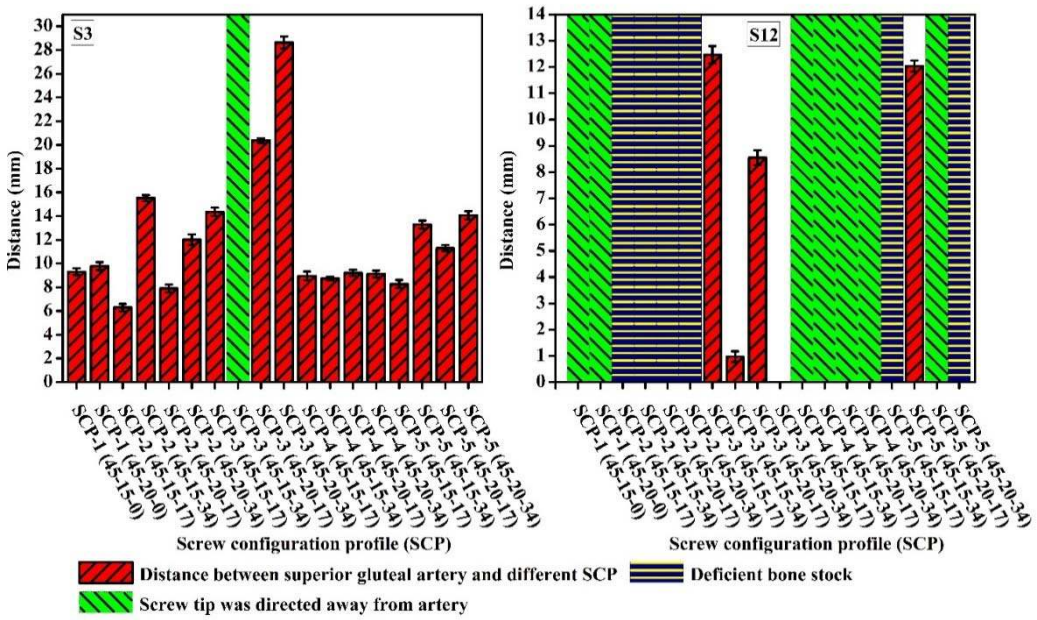

Figure 4.45: Graphs showing the distance measured from screw S3 and S12 to Superior gluteal artery

In addition, it was apparently not possible to show all eighteen possible ways of the each angulated screws pictographically. Therefore, we analyzed and engraved all structures with their respective criteria (i.e., C1, C2, C3, and C4) in tabular format Table 4.5.

Table 4.5: List of screws in all eighteen eccentric screw configuration profiles (SCP) following their respective criteria (i.e. C1, C2, C3, C4) relative to vessel structures proximal to pelvic bone.

	Obturator Artery				External Iliac Vein				External Iliac Artery				Inferior Gluteal Artery				Superior Gluteal Artery			
Screw Configuration Profile (SCP)	**C1**	**C2**	**C3**	**C4**	**C1**	**C2**	**C3**	**C4**	**C1**	**C2**	**C3**	**C4**	**C1**	**C2**	**C3**	**C4**	**C1**	**C2**	**C3**	**C4**
SCP-1 (45-15-0)	S4	S7		S0, S1		S5, S6, S8, S9				S6, S9	S5, S8			S0, S2, S3	S12			S3	S12	
SCP-1 (45-20-0)	S4	S7		S0, S1		S6, S8, S9	S5			S9	S5, S6, S8			S0, S2, S3	S12			S3	S12	
SCP-2 (45-15-17)	S4	S7		S0, S1		S6, S8, S9	S5		S8	S6, S9	S5			S0, S2, S12		S3		S3, 12		
SCP-2 (45-15-34)	S0, S4	S7		S1		S6, S9	S5	S8		S8	S5, S6, S9			S0, S2, S3, S12				S3, S12		
SCP-2 (45-20-17)	S4	S7		S0, S1	S9	S6, S8	S5		S9	S8	S5, 6 S			S0, S2, S3, S12				S3, S12		
SCP-2 (45-20-34)	S4	S7		S0, S1	S9	S6	S5	S8		S8	S5, S6, S9			S0, S2, S12		S3		S3, S12		
SCP-3 (45-15-17)	S4	S7		S0, S1		S6, S8		S5, S9	S8		S5, S6	S9		S0, S2, S3, S12				S3, S12		
SCP-3 (45-15-34)	S4	S7		S0, S1		S6	S8	S5, S9	S8	S5	S6	S9	S2	S0, S12	S3				S3	S12
SCP-3 (45-20-17)	S4	S7		S0, S1		S6, S9	S8	S5			S5, S6, S8	S9	S12	S0, S2	S3			S12	S3	
SCP-3 (45-20-34)	S4	S7	S0	S1		S6, S8		S5, S9	S8	S5, S9			S12		S0, S2, S3				S3	S12
SCP-4 (45-15-17)	S4	S7		S0, S1		S6, S8	S5, S9		S9	S6	S5, S8			S2, S3	S12	S0		S3	S12	
SCP-4 (45-15-34)	S0, S4	S7		S1	S9	S8	S5	S6	S9	S6	S5, S8			S2, S3	S12	S0		S3	S12	
SCP-4 (45-20-17)	S4	S7		S0, S1	S9	S6, S8	S5		S6, S8, S9		S5			S2, S3	S12	S0		S3	S12	
SCP-4 (45-20-34)	S0, S4	S7		S1	S9	S8	S5	S6	S9	S6, S8	S5			S0, S2	S3, S12			S3	S12	
SCP-5 (45-15-17)	S4	S7		S0, S1		S5, S6, S8, S9			S5, S6	S9	S8		S12	S0, S2		S3		S3, S12		
SCP-5 (45-15-34)		S7		S0, S1, S4		S5, S6, S8, S9			S6, S8	S9	S5		S12	S0, S2, S3				S3, S12		
SCP-5 (45-20-17)	S4	S7		S0, S1		S6, S8, S9	S5		S5, S6, S8	S9				S0, S2, S3	S12			S3	S12	
SCP-5 (45-20-34)	S4	S7		S0, S1		S6, S8, S9	S5		S5, S6, S8	S9			S12	S0, S2, S3				S3, S12		

4.16 Statistical analysis

we performed one-way analysis of variance (ANOVA) following with a post-Hoc Tukey's HSD test in graphing and analysis software Origin 9.1 (OriginLab Corporation, Northampton, USA). This test was performed to ascertain whether there was a statistically significant difference between the mean of rotated screw with ideal screw fixation (i.e., no eccentricity). We chose the significance level of .05 or below. Tables 4.6-4.10 below show a complete data of the analysis performed statistically.

Table 4.6: Statistical analysis data for Obturator artery

Obturator Artery					
Screw	**Ideal SCP (Group-1)**	**SCP (Group-2)**	**Mean Difference**	**P-Value**	**95% CL**
S0	SCP- 1	SCP-4 (45-20-34)	11.9998	<.0001	10.874 to 13.126
S1	SCP-1 (45-15-0)	SCP-3 (45-20-34)	3.1712	<.0001	2.5238 to 3.8186
S4	***ANOVA was not performed because all SCP had a good bone stock***				
S7	SCP-1 (45-20-0)	SCP-2 (45-20-17)	0.7630	=.3493	-0.0603 to 1.5865

Table 4.7: Statistical analysis data for External Iliac Vein

External Iliac Vein					
Screw	**Ideal SCP (Group-1)**	**SCP (Group-2)**	**Mean Difference**	**P-Value**	**95% CL**
S5	SCP-1 (45-15-0)	SCP-5 (45-20-34)	4.8808	<.0001	3.7537 to 6.008
S6	SCP-1 (45-15-0)	SCP-3 (45-20-34)	16.923	<.0001	15.421 to 18.425
S8	SCP-1 (45-15-0)	SCP-3 (45-15-34)	20.9305	<.0001	19.968 to 21.983
S9	SCP-1 (45-15-0)	SCP-2 (45-15-34)	13.3958	<.0001	12.422 to 14.37

Table 4.8: Statistical analysis data for External Iliac Artery

External Iliac Artery					
Screw	**Ideal SCP (Group-1)**	**SCP (Group-2)**	**Mean Difference**	**P-Value**	**95% CL**
S5	SCP-1 (45-15-0)	SCP-3 (45-20-17)	4.5140	<.0001	3.3376 to 5.6906
S6	SCP-1 (45-15-0)	SCP-3 (45-15-34)	14.9928	<.0001	14.16 to 15.826
S8	SCP-1 (45-20-0)	SCP-3 (45-20-17)	19.5615	<.0001	18.365 to 20.758
S9	SCP-1 (45-15-0)	SCP-2 (45-15-34)	17.7802	<.0001	16.804 to 18.757

Table 4.9: Statistical analysis data for Inferior Gluteal Artery

Inferior Gluteal Artery					
Screw	**Ideal SCP (Group-1)**	**SCP (Group-2)**	**Mean Difference**	**P-Value**	**95% CL**
S0	SCP-1 (45-20-0)	SCP-5 (45-20-17)	9.7836	<.0001	8.7891 to 10.778
S2	SCP-1 (45-20-0)	SCP-3 (45-20-34)	3.663	<.0001	2.7424 to 4.5836
S3	SCP-1 (45-15-0)	SCP-3 (45-20-17)	14.8016	<.0001	13.8083 to 15.8
S12	***ANOVA was not performed because in ideal condition screw lies inside bone.***				

Table 4.10: Statistical analysis data for Superior Gluteal artery

Superior gluteal artery					
Screw	**Ideal SCP (Group-1)**	**SCP (Group-2)**	**Mean Difference**	**P-Value**	**95% CL**
S3	SCP-1 (45-15-0)	SCP-3 (45-20-34)	19.3184	<.0001	18.128 to 20.509
S12	***ANOVA was not performed because in ideal condition screw lies inside bone.***				

4.17 Statistical Results

For obturator artery, screw S0 in SCP-4 (45-20-34) is statistically significant from ideal screw fixation (SCP- 1) ($P < .0001$). Screw S1 in SCP-3 (45-20-34) has the most significant difference ($P < .0001$) from SCP-1(45-15-0). We did not test the significance level in screw S4 because, in ideal SCP, the screw had a good bone stock. Screw S7 in SCP-2 (45-20-17) was not statistically different ($P=.3493$) from SCP-1 (45-20-0) and both lie in criteria C3 (Table 4.6).

External iliac vein lies in anterior quadrant encountered with screws S5, S6, S8, and S9 (Figure 3). Screw S5 in SCP-5 (45-20-34) having most significant difference ($P< .0001$) among all eccentric profiles, follows criteria C1. Screw S6 in SCP-3 (45-20-34) was significantly different ($P< .0001$) from ideal SCP and follows criteria C3 because of less bone stock. Screw S8 in SCP-3 (45-15-34) (45-20-17) (45-20-34) has most significant difference ($P< .0001$) with ideal SCP. SCP-3 (45-15-34) (45-20-17) follows criteria C1 and SCP-3 (45-20-34) follows criteria C3 due to insufficient bone stock. Screw S9 in SCP-2 (45-15-34) having most significant difference ($P< .0001$) with ideal SCP, follows criteria C3 because of less bone stock (Table 4.7).

The external iliac artery was adjacent to the anterior column and was found close to screws S5, S6, S8 and S9 (Figure 3). Screw S5 in SCP-1 (45-15-0) was significantly different ($P< .0001$) from SCP-3 (45-15-17) and lies in criteria C1. Screw S6 in SCP-3 (45-15-34) is statistically different ($P< .0001$) with ideal SCP, and lies in criteria C1. Screw S8 in SCP-3 (45-20-17) was having a significant difference ($P < .0001$) with ideal SCP and follows

criteria C1. Screw S9 in SCP-2 (45-15-34) is statistically different (P< .0001) and lies in criteria C1 (Table 4.8).

Inferior gluteal artery found closer to the posterior column, encountered with S0, S2, S3, and S12 screws (Figure 3). Screw S0 in SCP-5 (45-15-17) has the significant difference (P< .0001) but lies in C3 because of deficient bone stock. Screw S2 itself was most significant (P < .0001) from SCP-5 (45-15-17), followed criteria C3 because of less bone stock. Screw S3 in SCP-3 (45-20-17) is statistically different from ideal SCP (P< .0001) and lies in criteria C1. We did not perform any statistical analysis for screw S12 as the ideal screw lies inside the pelvic bone (Table 4.9).

Superior gluteal arteries were close to the pelvic bone at the superior portion of the sciatic notch in the posterior quadrant and encountered with S3 and S12 screws (Figure 3). Screw S3 in SCP- 3(45-20-17) was statistically different (P< .0001) from ideal SCP and lies in criteria C1. Statistical analysis was not performed for screw S12 because ideal SCP has the absolute bone stock (Table 4.10).

4.18 Discussion and Conclusions

Researchers have published various reports on vascular injuries by placement of screws in context with total hip arthroplasty; they are particularly dangerous since they can lead to the elimination or even to the death of the patient (C.R. Wheeless, 2016; B. Nachbur 1979; M.A. Reiley et al, 1984; A.S. Haveson et al, 1990) Preventing the vascular complications during total hip arthroplasty is the most important aspect of treatment. In addition, external iliac vessel and obturator artery seems to have been the most frequent injury because of

their close proximity to the anterior column and quadrilateral surface respectively. N A. Shoenfeld et al showed that location of the external iliac artery directly medial to the pubic component of the acetabulum places this vessel at risk of injury with drilling or reaming maneuvers. In so doing, thrombosis may occur as a result of the exothermic reaction and result in perforation and pseudoaneurysm formation. These vessels are vulnerable to avulsion if a revision procedure becomes necessary. Therefore, for patients with vessels at risk, a preliminary retroperitoneal exposure of the external iliac vessels is advised before extraction of the acetabular component to prevent life-threatening hemorrhagic complications associated with lacerations or avulsions of these vessels. C. J. Lavernia et al performed an anatomical study on surgical treatment of neurovascular injury during reconstruction of acetabular cage and reported that a cavitary defect was cut out in the acetabulum and a cage was placed in each of ten hemipelvises (J. Lavernia et al, 2007). The comparative progression of the neurovascular bundle of superior gluteal nerve was observed to evaluate dissection gaps. When cage screws of approximate length of 15 mm longer than required were positioned, 13% of the superior flange screws and 20% of anterior rim screws hit the femoral nerve. Approximately 60% of posterior rim screws threatened the obturator nerve. Therefore, they considered a safe zone for the screw size that might be 15 mm for the superior flange and 25mm for the posterior rim. However, injury to internal iliac vessel, inferior and superior gluteal vessel also has been reported (M. Marmor et al, 2010; Y. Kawasaki et al., 2012; E. L.M. Kong et al, 2013).

Wasielewski et al. precisely described the quadrant system to prevent vascular as well as neural structure, proximal to the pelvic bone. They suggested the use of the quadrant system for placement of screws in cementless cup fixation, and hip arthroplasty surgeons already accepted it widely until date. In recent years, optimizing the total hip component, manufacturers are providing the eccentric hole (up to 34°) for screw fixation in acetabular cup, which may perhaps not abide the quadrant system provided by Wasielewski et al. However, we are aware of no similar reports (to our knowledge) on effect of angular eccentric screws on vascular injury. In spite of this work, Jui-Ting Hsu et al. had carried out mechanical study effect of press fit cup along with offset and angular eccentric screw in different experimental as well in the computational environment which is not directly associated with these findings (J. Hsu et al, 2007; J.T. Hsu et al, 2007). Thus, we sought to determine the effect of the eccentric screw for two angular rotation angle (17° and 34°), along with different configuration (Table 4.2).

The study used computed tomography angiography scans and special medical imaging, editing software Mimics18.0 to reconstruct the osseous, and vessel structures of the pelvis. We also determined the distance between the intrapelvic blood vessels and impeding screw, following criteria C1, C2, C3, and C4 by Creo 3.0 parametric analysis tool.

From the results of the surgical simulation, measurements, and statistical analysis, it is evident that eccentric screws play a vital role in the vascular injury. Considering quadrant system (proposed by Wasielewski et al.) and our findings, the polar position is rarely used position for a screw, because of deficient bone stock and presence of obturator artery. Thus,

we can conclude that screws that were lying in the polar position were potentially dangerous for obturator artery. Visual determination provided that few screws, which lie in anterior or posterior quadrants in ideal fixation, they were directed towards polar positions due to angular rotation, and thus felt in the dangerous category for vessel structures.

Screws that lie in the posterior superior quadrant are not directed to the external iliac vessels or obturator artery. In addition, some of SCP of the screws like S10 of profile SCP-5 (45-15-17) (45-20-17), SCP-4 (45-15-34) (45-20-34), SCP-2 (45-15-17) (45-20-17) (45-15-34) (45-20-34), SCP-1 (45-15-0) (45-20-0) and S4 of profile SCP-4 (45-15-17) (45-20-17) (45-15-34) (45-20-34) and screw S11 of profile SCP-3 (45-15-34) (45-20-34) are not significant for use due to deficient bone stock. Despite this, screws that lies in posterior superior quadrant or screws directed to the posterior superior quadrant for the rationale of eccentricity and square measure significantly safe.

Screws directed towards the posterior inferior quadrant, lie close to the superior and inferior gluteal artery and pudendal artery, and yet are entirely safe in the vast majority of the angular eccentric profile (Table 4.2). S11 might be downright insulted screw because of insufficient bone stock from transition zone of line-B (Figure 4.38) to the distal portion of the posterior quadrant.

The study addresses the critical issue of screws placed in an anterior quadrant in different eccentric SCP. Screws that lie in superior anterior quadrant or screws directed because of eccentricity occur in proximity to the external iliac vein and artery. However, external iliac

vein is more medial, or close proximal to the polar surface, the eccentric profile or ideal fixation of screws in the anterior quadrant are possibly unsafe.

Angulated screws, laying in anterior inferior quadrant or screws originating from other quadrant, but they are directed to anterior inferior quadrant are potentially dangerous for obturator artery. In this quadrant, the bone purchase was significantly less in a majority of the subject.

In general, major outcome of our study indicates that quadrant system represented by Wasielewski et al. was slightly different in relation to the modern prosthetic cup with the eccentric hole for screw fixation. Additionally, screws that were found probably dangerous for vessel structures in Wasielewski findings could be significantly tolerable and benefited for due consideration as a result of angular eccentricity.

The study subjects to a few limitations. To start with, we performed the study only on an Indian populace, and the stature of the subjects was fairly short. We did not examine the results with other populace, for example, in the Japanese, Chinese, Africans, US, and Europe.

Secondly, we did not investigate patients with the hip disease such as osteoarthritis, rheumatoid arthritis. Therefore, our results may not apply to all patients with hip disease. We however, believe that the present data apply to patients with the hip disease because patients requiring THA are generally older and have atrophy of the muscles around the hip joint due to disuse.

Thirdly, neural structures were not identifiable in angiographic computed tomography. In most cases, these nerves keep company with the homonymous blood vessels in the neurovascular bundle. Along these lines, we are inclined to believe that a safe or dangerous zone for eccentric screws characterized by the vascular structures might be used likewise to avoid injury to nerves.

Lastly, we did not perform study on the aberrant anatomy of vessel structures and developmental dysplasia of hip (M.M. Pai et al, 2009; V.I. Sakellariou et al, 2014; R. Narasimhan, 2003; F.D. Angelo et al, 2008). However, in our thirty-eight subject's data no anatomical variants and dysplasia of hip were present.

In conclusion, cementless cup with screw fixation in minimally invasive total hip arthroplasty is technically demanding. We trust that the data concerning the placement of eccentric screws in modern cup may be helpful in avoiding neurovascular injury. Further, the surgeons must consider the operating procedure to guarantee the safe screw placement with the angular eccentric profile of hole in the prosthetic cup.